UNIVERSIDAD TÉCNICA FEDERICO SANTA MARÍA
DEPARTAMENTO DE FÍSICA
VALPARAÍSO - CHILE

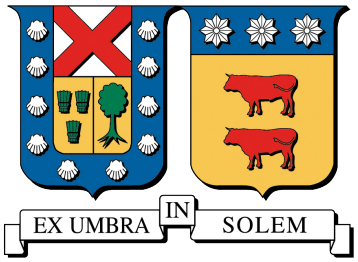

RENORMALON MOTIVATED EVALUATION OF THE BJORKEN SUM RULE AT LOW MOMENTA

CAMILO NICOLÁS CASTRO ARRIAZA

THESIS SUBMITTED AS REQUIRED FOR THE DEGREE OF
MASTER OF SCIENCE IN PHYSICS

ADVISOR	:	**DR. GORAZD CVETIČ**
CO-ADVISOR	:	**DR. CÉSAR AYALA (UTA)**
EXAMINATION COMMITTEE	:	**DR. MARAT SIDDIKOV (UTFSM)** **DR. ALFREDO VEGA (UV)**

JANUARY 2024

"For a long time, science and technology have made it possible to assure that everybody enjoys those basic necessities which today are enjoyed only by a minority. The difficulties are not technical, and - in our case at least - they are not due to a lack of national resources. What prevents the realisation of our ideals is the organisation of society, the nature of the interests which have so far dominated, the obstacles which dependent nations face. We must concentrate our attention on these structures and on these institutional requirements"

Salvador Allende Gossens, 1970.

Acknowledgements

I would like to thank my advisor Prof. Gorazd Cvetič and my coadvisor Dr. César Ayala for allowing me to participate in this research project and for always treating me so respectfully and patiently. It has been an honour to work with Prof. Cvetič in these topics since my undergraduate degree, and I'll always be thankful for how much knowledge he has given me these years.

I also want to express my gratitude to the professors in the examination committee whom I made wait for so long to read this work for their patience and disposition.

I want to thank my parents and sister for their never-ending love, patience, and support for me throughout my life, and how they have always motivated me to do my best and persevere in all my (often ill-advised) projects.

I must give a special acknowledgement to my dearest Valentina, who has been by my side in many ways through the years, and who has long supported me with love and companionship especially through the difficulties of writing this work.

Finally, I'd like to thank my dear academic cohort friends Amanda, Pablo (thank you for our shared desk discussions too!), and Sofi, who have been with me for so long, the process of the undergrad and Master's was infinitely better with you near.

The development of this thesis was supported by FONDECYT project nº 1220095.

Contents

Chapter 1

Introduction and Concepts

In the context of the Standard Model of Particle Physics, Quantum Chromodynamics (QCD) is the gauge field theory which describes the strong colour interaction between quarks mediated by gluons. In the internal symmetry structure of the Standard Model, $SU(3)_c \times SU(2)_L \times U(1)_Y$, QCD is the SU(3) colour component, with quarks therefore being in the fundamental representation of the $SU(3)_c$ group.

The development of a formal theory for the strong interaction, in view of the great quantity of non-fundamental hadrons discovered thus far, began in the sixties with the proposal by M. Gell-Mann [1] and G. Zweig [2] of the existence of three flavours of fundamental particles that would form hadrons: quarks. This suggested that objects bound by the strong interaction are all formed by quarks and, after the discovery of these, it remained to formulate a full theory that described their dynamics and the workings of colour charge. It was in this context that, in 1973, Fritzsch, Gell-Mann, and Leutwyler proposed [3] a gauge field theory that fulfilled precisely this role, Quantum Chromodynamics (QCD).

The main predictive method for the evaluation of QCD observables is the use of perturbative expansions (pQCD), due to the asymptotic freedom exhibited by the theory. This characteristic, discovered by D. Gross and F. Wilczek [4] and independently by H. D. Politzer [5], allows the use of perturbation theory with relative ease and accuracy for quantities at high energies but becomes a problem at lower energies where perturbation theory is not valid due to the strength of the interaction. This forces us to use other, non-perturbative, methods for predictions at low energies, of which there are many ranging from lattice gauge theory and numerical simulations

to analytic methods that make corrections to perturbative calculations.

A very important and well-studied spacelike QCD observable is the Bjorken Sum Rule (BSR) [6, 7], which relates the structure functions of the proton and neutron, due to it being the archetype of QCD spin sum rules and thus being key in the study of nucleon spin structure and, thanks to the great wealth of data available for it in a wide energy range, being a good candidate for use in testing non-perturbative approaches to QCD.

In this work we study a specific method for the evaluation of QCD observables, developed by G. Cvetič in [8], based on the renormalon structure known for many observables and that uses it to generate a resummation of such quantities valid in the region of low energies not usually accessible through pQCD only. In particular, the main objective here is to apply the Cvetič approach to the inelastic polarised Bjorken Sum Rule (BSR) to get predictions through resummation. The main contribution of this thesis (found in Chapter 3) is that it contains and expands on many of the procedures and calculations that form the basis for our two recent articles, one already published [9] and one in still in refereeing [10], and in addition summarises and comments on the results from our articles.

First though, it is necessary to give a brief introduction to some of the concepts that will later arise in this work to better understand the challenges inherent to pQCD at low energies and how these motivate the method we chose to apply.

1.1 The QCD Coupling

In the QCD lagrangian

$$\mathcal{L} = \sum_q \bar{\psi}_{q,a}(i\gamma^\mu \partial_\mu \delta_{ab} - \sqrt{4\pi\alpha_s}\gamma^\mu t^C_{ab}\mathcal{A}^C_\mu - m_q\delta_{ab})\psi_{q,b} - \frac{1}{4}F^A_{\mu\nu}F^{A\ \mu\nu}, \tag{1.1}$$

α_s is the coupling that encodes the strength of the interactions of quarks and gluons. The dependence of $\alpha_s(Q^2)$ (where $Q^2 \equiv -q^2$) on momentum transfer Q thus underlies the behaviour of such particles at different regimes, from colour confinement at low momentum transfer (low energies, long distance, the infrared regime) to

asymptotic freedom at high momenta (high energies, short distance, the ultraviolet regime). As such, it is necessary to understand the coupling over that entire range to describe hadron physics in both regimes.

Thanks to the anti-screening effect caused by gluons that dominates over the screening effect from quark-antiquark loops, the QCD running coupling tends to decrease with increasing Q^2, thus bringing about what is known as the asymptotic freedom of the theory [4, 5], which means that the interaction between particles decreases as the energy scale increases. Due to this, much of the evaluation of observables can be done accurately with perturbation theory, since we can just make perturbative expansions on the coupling, but this stops working for lower energies where the coupling grows large.

When working in perturbative QCD (pQCD), we express predictions in terms of a renormalised version of the coupling $\alpha_s(\mu^2)$, which is a function of an unphysical renormalisation scale μ according to a given prescription from a renormalisation scheme (RS). Despite this, we know the observables themselves must be independent of the renormalisation scheme, which means the series coefficients will be RS-dependent in some way. This can be seen in the renormalisation group equation (RGE) which the renormalised coupling satisfies

$$\mu^2 \frac{d\alpha_s}{d\mu^2} = \beta(\alpha_s) = -(b_0\alpha_s^2 + b_1\alpha_s^3 + b_2\alpha_s^4 + \dots), \tag{1.2}$$

where $b_{0,1,2,\dots}$ are the β-function coefficients that depend on n_f, the number of interacting quark flavours we will consider for our process in contrast to the heavier remaining ones that decouple from the theory, and on the renormalisation scheme parameters (though only from the 3-loop coefficient (b_2) onwards). In addition, the minus sign in Eq. (1.2) codifies the fact that the coupling becomes weak for large Q^2, i.e. it exhibits the asymptotic freedom previously described.

It is important to note that the behaviour of the pQCD coupling when approaching the IR regime includes not only growth (as would be expected from asymptotic freedom), which in itself precludes the use of perturbation theory at such energies, but also predicts the appearance of unphysical Landau singularities at low Q^2 where the coupling becomes infinite, which appears outside the validity of pQCD itself and thus is not a valid prediction but an artifact of pQCD arising from its lack of non-perturbative contributions. It must be stressed that these Landau singularities and

thus the divergence of the pQCD α_s is not what causes quark confinement as was once thought, since such an assumption ignores that the singularities are unphysical and that the perturbative approach does not include long distance effects that are important in the IR regime. For more details on the coupling see reviews such as those in Refs. [11, 12].

1.2 Divergent Series and the Limits of pQCD

The use of perturbation theory when modelling QCD observables is permitted (for high energies at least) by the asymptotic freedom exhibited by this theory. As mentioned earlier, this property means that, in QCD, the interaction between particles tends to become asymptotically weaker as the energy scale increases, and thus the running coupling $a(\mu^2)$ ($\equiv \alpha_s(\mu^2)/\pi,\ \mu^2 = \kappa Q^2$) becomes smaller the higher we go up the energy scale. This idiosyncratic behaviour is what permits the use of a finite number of terms in the perturbative expansion of the observables we want to evaluate to get reasonable predictions.

It is this very characteristic that brings about the rather unwelcome effect at low energies that, due to the fact that the interaction (and thus the coupling) becomes strong in this region, we can no longer use perturbation theory for our calculations. Moreover, in the usual perturbative QCD approach, the coupling has Landau singularities in the positive semiaxis $0 \leq Q^2$ in the low energy region $Q^2 \lesssim \Lambda^2 \sim 1\ \text{GeV}^2$, which means that evaluating or making transforms on spacelike observables $d(Q^2)$ with this coupling will lead to such singularities in the observables too at low Q^2. This is in direct opposition to general QFT principles which imply that these observables should be holomorphic functions. Apart from this, the singularities that would appear in the evaluation observables when $a(Q^2)$ is near or in the region of the Landau singularities would render the necessary integrals unreliable or impossible to compute due to the ambiguity introduced.

Not only must we consider the coupling though, since we can see that in any generic power series that serves as a general way of expressing QFT observables

$$R = \sum_n r_n \alpha^n, \tag{1.3}$$

given in powers of the renormalised coupling α, the series is nearly always divergent independently of α. This is because the expansion coefficients have been found to have the form

$$r_n \overset{n\to\infty}{\sim} K a^n n! n^b, \tag{1.4}$$

and thus diverge at high n. This unphysical divergence of the series for the observable, suggests some non-trivial and non-perturbative contributions are missed when using this approach. Indeed, simply using further terms in Eq. (1.4) does not improve the approximation of R beyond a certain point so, having no non-perturbative form for R, we must somehow sum the divergent series to actually improve the approximation. A way of doing so is with Borel summation, where we define the Borel transform of $R \sim \sum_{n=0}^{\infty} r_n \alpha^{n+1}$ as

$$\mathcal{B}[R](t) = \sum_{n=0}^{\infty} r_n \frac{t^n}{n!}. \tag{1.5}$$

If $\mathcal{B}[R](t)$ is well behaved, we can define

$$\tilde{R} = \int_0^{\infty} dt\ e^{-\frac{t}{\alpha}} \mathcal{B}[R](t) \tag{1.6}$$

which, if it exists, thus provides the Borel sum of the series R.

The Borel transform and integral are considered phenomenologically useful, since it has been found that the Borel transform can be understood as the generating function of the coefficients r_n, which thus means that singularities (such as renormalons) in the Borel plane are related and somehow encode the inherent divergence of the original series.

1.3 Renormalons

Renormalons are a kind of divergence that arise in the Borel transforms and integrals of QCD observables due to its high or low momentum behaviour. They were originally found in certain bubble diagram contributions to correlators [13–15] such as those in Fig. 1.1 for the Adler function, but these types of divergence are not exclusive to

such diagrams, which are presented here only illustratively.

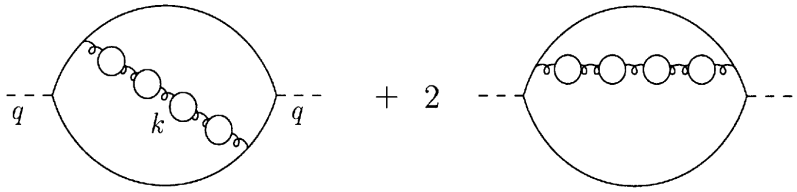

Figure 1.1: Bubble diagrams for the Adler function from which its UV and IR renormalons can be derived. These are all the diagrams with fermion loops inserted in a gluon line. Diagrams come from the renormalon review work by Beneke [16] mentioned in the text.

Renormalons are thus a source of divergence in the Borel plane when summing a divergent series from a QCD observable that has singularities. The knowledge of the location of singularities for different observables in the Borel plane can then be used to generate a resummation of the dominant part of their series expansion that contain more information than simple truncation of the original series, an idea that motivates the method chosen for this work. For more technical details on renormalons and their connection to different phenomenological methods, see Ref. [16].

It is important to note that the emergence of renormalon divergences is unrelated to the Landau singularities that arise in the pQCD coupling, because renormalons appear independent of the coupling used.

1.4 Polarised Bjorken Sum Rule

The polarised Bjorken Sum Rule (BSR) $\Gamma_1^{p-n}(Q^2)$ [6, 7] is the difference between the polarised structure functions g_1 of the proton and neutron integrated over the Bjorken scaling variable x. Of particular interest is the inelastic part (note the bar over Γ) of the sum rule

$$\bar{\Gamma}_1^{p-n}(Q^2) = \int_0^{1^-} dx\ [g_1^p(x,Q^2) - g_1^n(x,Q^2)], \tag{1.7}$$

since it can be (and is) obtained from the measurements in deeply inelastic scat-

tering (DIS) processes of the spin-dependent structure functions, such as in DI lepton-nucleon scattering experiments. A great wealth of such results from different experiments are available from CERN [17], DESY [18], SLAC [19], and Jefferson Lab [20–23], with various values of x and over a wide range of momentum transfer $Q^2 \equiv -q^2$ (from 0.02 GeV^2 up to 5 GeV^2) as can be seen in Fig. 1.2 from [9]. This availability of experimental data motivates the use of the BSR to test the results of different evaluation methods for QCD at low Q^2, as is the case in this work, both for comparing to the data and because of the possibility of enhancing our predictions by performing fits to it.

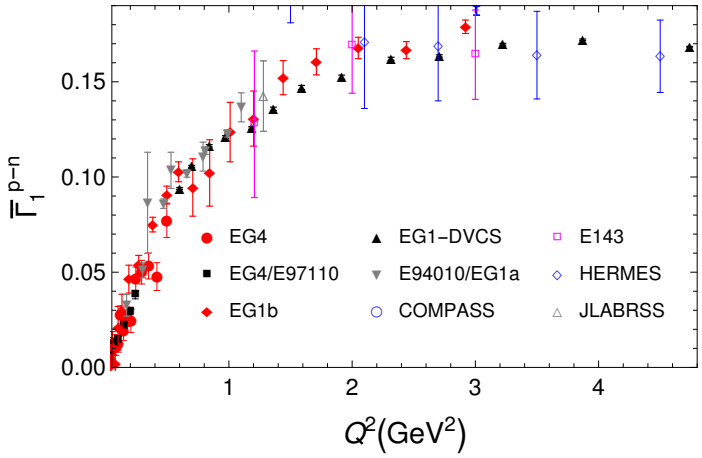

Figure 1.2: Experimental Values for the polarised inelastic BSR $\bar{\Gamma}_1^{p-n}(Q^2)$ based on the data from different experiments [17–23] shown with statistical uncertainties. Figure from [9] by C. Ayala, G. Cvetič & C.C.A.

The BSR has a theoretical Operator Product Expansion (OPE) in the form [6, 7]

$$\bar{\Gamma}_1^{p-n,\mathrm{OPE}}(Q^2) = \left|\frac{g_A}{g_V}\right|\frac{1}{6}(1 - d(Q^2)) + \sum_{i=2}^{\infty} \frac{\mu_{2i}(Q^2)}{Q^{2i-2}}, \tag{1.8}$$

where $|g_A/g_V| = 1.2754$ is the ratio of the nucleon axial charge, and $d(Q^2)$ is the canonical zero-dimension QCD part that has a known perturbation series expansion in powers of the pQCD coupling:

$$d(Q^2)_{\mathrm{pt}} = a(Q^2) + d_1 a(Q^2)^2 + d_2 a(Q^2)^4 + d_3 a(Q^2)^4 + \mathcal{O}(a^5). \tag{1.9}$$

Here, $d_0 = 1$, and the next three coefficients $d_{1,2,3}$ are known exactly [24–26]

at least for the $\overline{\text{MS}}$ scheme, also $n_f = 3$ is taken throughout this work. For the d_4 coefficient there is an estimation made with the Effective Charge (ECH) method that will be used in this work where $d_4 = 1557.4$, once again for the $\overline{\text{MS}}$ scheme. Knowing the coefficients in the $\overline{\text{MS}}$ scheme is sufficient for our purposes since we can find explicit transformations for them from one renormalisation scheme prescription to any other, which we will present later in this thesis. Though it is usual for the BSR to be evaluated in pQCD with $d(Q^2)_{\text{pt}}$ truncated, we know that the expansion coefficients d_n grow very fast with increasing n, so merely truncating the perturbative series may miss important contributions.

The $D = 2$ term in the OPE Eq. (1.8) has a known Q^2 dependence

$$\frac{\mu_4(Q^2)}{Q^2} = \frac{M_N^2}{9}\frac{\left[(a_2^{p-n} + 4d_2^{p-n}) + 4\bar{f}_2\, a(Q^2)^{k_1}\right]}{Q^2}, \tag{1.10}$$

where $k_1 = 32/81$ is the anomalous dimension, $M_N = 0.9389$ is the nucleon mass and $(a_2^{p-n} + 4d_2^{p-n}) \approx 0.063$. $\bar{f}_2$ however is not known, but can be fitted as a parameter from experimental values that exist for Eq. (1.7). This is also the case for the whole $D = 4$ OPE term, which is not theoretically known but can reasonably be taken as independent from Q^2 and then fit its coefficient μ_6 to the data.

1.5 Holomorphic versions of QCD (AQCD)

Because of the Landau singularities that appear in the pQCD coupling that were mentioned in Sections 1.1 & 1.2, there have been many different methods proposed for the evaluation of observables in the regime where $0 < Q^2 \lesssim 1$ GeV^2 apart from truncation of the perturbative series (TPS), such as specific low-Q^2 models [20, 27, 28], while others are based on the replacement of the pQCD coupling by some form of different $\mathcal{A}(Q^2)$ coupling that has no Landau singularities.

The latter methods are alternatives called holomorphic or analytic versions of QCD (AQCD), variants in which the coupling has no unphysical Landau singularities and thus is holomorphic for all non-negative Q^2, and also practically coincides with the pQCD coupling for high Q^2, which in this way alleviates the ambiguity problem that observable evaluation has in the low momentum transfer region.

Many AQCD models gave been proposed, starting with the work by D.V. Shirkov

and I.L. Solovstov [29]. The idea of the different AQCD methods is that we can also impose other conditions on the coupling so that it is beneficial for the evaluation of physically relevant observables.

Though not the focus of this thesis, in our recent work [9, 10] we employ (apart from the fundamental pQCD) two specific AQCD versions because they eliminate the ambiguities in the evaluation of the canonical part $d(Q^2)$ of the BSR, these are 2δAQCD, developed in [30], and 3δAQCD, developed in [31, 32]. The details of the construction of these AQCD variants for our purposes are omitted in this thesis since we just present the results for comparison, but they can be found in Appendix F from [10]. The important thing to understand is that the couplings used when working with 2δAQCD and 3δAQCD are proved to not have Landau singularities and coincide with the underlying pQCD coupling at high Q^2 while constrained by certain physically motivated conditions, all under many different renormalisation schemes, and thus we can justifiably repeat all the steps of the Cvetič method developed for the pQCD coupling with the corresponding AQCD couplings with no problems. We make reference to the incidence of the renormalisation scheme on the AQCD couplings occasionally in this work, but all further details on this behaviour can be found in [10].

More information on AQCD, descriptions, and comparisons of different methods can be found in the review from Ref. [33].

1.6 Desirable Conditions for Evaluating Observables

In summary, in order to evaluate observables in the $|Q^2| \lesssim 1$ GeV^2 region and get reliable, unambiguous predictions:

- Since the exact coefficients $d_n(\kappa)$ of the perturbative series of $d(Q^2)$ are not known, except for the first few, we desire a way to get good, and preferably physically motivated, approximations for these coefficients at any n.
- Given that, even if we know all the coefficients d_n or have an approximation for them, the perturbation series of the observable $d(Q^2)$ is still necessarily asymptotically divergent (both in pQCD and AQCD) due to the renormalon

divergence of the coefficients, we need a way to make the evaluation of the observable despite such divergence.

- Since in pQCD the coupling $a(\kappa Q^2)$ has Landau singularities at low momentum transfer values, which makes the evaluation ambiguous, it is desirable that we work with a coupling that lacks such singularities outside of the negative semiaxis.

In addition to these three conditions, it is also desirable that the results from a chosen method coincide with the usual pQCD approach for high energies.

Chapter 2

Outline of the Cvetič Method

Given the many problems that pQCD exhibits in low energy regimes mentioned in the previous chapter, we will now introduce a different approach to the evaluation of observables in this regime, which was developed by G. Cvetič in [8], and is the one chosen for evaluating the BSR (as will be done in the next chapter) in the published work this thesis complements. This method of evaluation of QCD observables is based on the renormalon structure of these, and relies on rewriting the usual perturbative power expansion of $d(Q^2)$ and then making a renormalon motivated *ansatz* for the Borel transform of such rewritten quantity. With this, a characteristic function is then found, which is used to evaluate the observable through resummation. The approach allows that what is obtained for the leading-twist canonical part can then be enhanced phenomenologically by making fits to the available data for the corresponding observable while including the higher-twist OPE terms.

2.1 Construction of Expansion Series and Borel Transforms

Since we want to model the renormalon structure of an observable in a more convenient way, we start by constructing a rewritten expansion series for the observable. Let the usual perturbative expansion of a QCD observable $d(Q^2)$, in powers of the renormalised coupling $a(\mu^2)$ where $\mu^2 = \kappa Q^2$ $(0 < \kappa \lesssim 1)$ in a chosen renormalisation scale, be

$$d(Q^2)_{\text{pert}} = a(\kappa Q^2) + d_1(\kappa)a(\kappa Q^2)^2 + \cdots + d_n(\kappa)a(\kappa Q^2)^{n+1} + \dots \tag{2.1}$$

Here we must note that, even though $d(Q^2)$ itself is κ-independent due to it being an observable, its expansion terms are not. The Borel transform of $d(Q^2)$ is thus the generating function of the perturbation coefficients d_n in Eq. (2.1):

$$\mathcal{B}[d](u;\kappa) \equiv 1 + \frac{d_1(\kappa)}{1!\beta_0}u + \ldots + \frac{d_n(\kappa)}{n!\beta_0^n}u^n + \dots \tag{2.2}$$

And its inverse Borel transform is then

$$d(Q^2) = \frac{1}{\beta_0}\int_0^\infty du \exp\left[-\frac{u}{\beta_0 a(\kappa Q^2)}\right]\mathcal{B}[d](u;\kappa) \tag{2.3}$$

Instead of the usual perturbative expansion from Eq. (2.1) in powers of $a(\kappa Q^2)$, we can write a series based on logarithmic derivatives $\tilde{a}_n(\kappa Q^2)$ instead in the form

$$\tilde{a}_n(\mu^2) \equiv \frac{(-1)^{n-1}}{(n-1)!\beta_0^{n-1}}\left(\frac{d}{d\ln\mu^2}\right)^{n-1} a(\mu^2), \tag{2.4}$$

where $(n = 0, 1, 2, \dots)$ and $\beta_0 = (11 - 2n_f/3)/4$, which for $n_f = 3$ gives $\beta_0 = 9/4$, is the first β-coefficient in the renormalisation group equation (RGE) in any chosen renormalisation scheme

$$\frac{da(\mu^2)}{d\ln\mu^2} \equiv \beta(a(\mu^2)) = -\beta_0 a(\mu^2)^2 - \beta_1 a(\mu^2)^3 - \beta_2 a(\mu^2)^4 - \dots \tag{2.5}$$

$$= -\beta_0 a(\mu^2)^2(1 + c_1 a(\mu^2) + c_2 a(\mu^2)^2 + \dots). \tag{2.6}$$

Here, the higher β-coefficients are replaced with the coefficients $c_j \equiv \beta_j/\beta_0$; the latter, for $j \geq 2$, characterise the renormalisation scheme and thus describe the RS-dependence. We need now to rewrite the series from Eq. (2.1) with the logarithmic derivatives from Eq. (2.4), by first rewriting the logarithmic derivatives in Eq. (2.4) in powers of a^n using the RGE in Eq. (2.5) which gives:

$$\tilde{a}_n(Q^2) = a(Q^2)^n + \sum_{m=1}^{\infty} k_m(n)a(Q^2)^{n+m}. \tag{2.7}$$

Or, when inverted:

$$a(Q^2)^n = \tilde{a}_n(Q^2) + \sum_{m=1}^{\infty} \tilde{k}_m(n)\tilde{a}_{n+m}(Q^2). \tag{2.8}$$

Here, the coefficients $k_m(n), \tilde{k}_m(n)$ depend only on the RGE coefficients c_j and are renormalisation scale μ^2 independent. The expressions Eq. (2.8) have the explicit form:

$$\begin{gathered} a^5 = \tilde{a}_5 + \ldots, \; a^4 = \tilde{a}_4 - \frac{13}{3}c_1\tilde{a}_5 + \ldots, \\ a^3 = \tilde{a}_3 - \frac{5}{2}c_1\tilde{a}_4 + \left(-3c_2 + \frac{28}{3}c_1^2\right)\tilde{a}_5 + \ldots, \\ a^2 = \tilde{a}_2 - c_1\tilde{a}_3 + \left(-c_2 + \frac{5}{2}c_1^2\right)\tilde{a}_4 + \left(-c_3a^5 + \frac{22}{3}c_1c_2 - \frac{28}{3}c_1^3\right)\tilde{a}_5 + \ldots, \text{ etc.} \end{gathered} \tag{2.9}$$

Additionally, $\tilde{a}_1 = a$. With these, we can now write the perturbative expansion from Eq. (2.1) as

$$d(Q^2)_{\log} = a(\kappa Q^2) + \tilde{d}_1(\kappa)\tilde{a}_2(\kappa Q^2) + \tilde{d}_2(\kappa)\tilde{a}_3(\kappa Q^2) + \cdots + \tilde{d}_n(\kappa)\tilde{a}_{n+1}(\kappa Q^2) + \ldots, \tag{2.10}$$

where we have new expansion coefficients $\tilde{d}_n(\kappa)$. It can easily be seen that these are related to the original d_n (noting that $\tilde{d}_0 = 1$), omitting the κ-dependence for simplicity of notation, as

$$\tilde{d}_n = \sum_{s=0}^{n-1} \tilde{k}_s(n+1-s)d_{n-s}, \tag{2.11}$$

or, inversely:

$$d_n = \sum_{s=0}^{n-1} k_s(n+1-s)\tilde{d}_{n-s}, \tag{2.12}$$

where the coefficients $\tilde{k}_s, k_s$ are the same as those that appear in Eqs. (2.7), (2.8). It is important to know these coefficients explicitly, so we reproduce here some of

these according to Eq. (2.11)

$$\begin{aligned}
\tilde{d}_0 &= d_0 = 1, \quad \tilde{d}_1 = d_1, \quad \tilde{d}_2 = d_2 - c_1 d_1, \\
\tilde{d}_3 &= d_3 - \frac{5}{2} c_1 d_2 + \left(-c_2 + \frac{5}{2} c_1^2 \right) d_1, \\
\tilde{d}_4 &= d_4 - \frac{13}{3} c_1 d_3 + \left(-3c_2 + \frac{28}{3} c_1^2 \right) d_2 + \left(-c_3 + \frac{22}{3} c_1 c_2 - \frac{28}{3} c_1^3 \right) d_1,
\end{aligned} \tag{2.13}$$

and so on. These can also be inverted accordingly to express the coefficients d_n in terms of $\tilde{d}_n$. Having now explicit forms for the coefficients $\tilde{d}_n(\kappa)$ from Eq. (2.11) we can take Eq. (2.10) and replace $\tilde{a}_n(Q^2) \mapsto a(Q^2)^n$ and thus construct the quantity

$$\tilde{d}(Q^2;\kappa) = a(\kappa Q^2) + \tilde{d}_1(\kappa) a(\kappa Q^2)^2 + \tilde{d}_2(\kappa) a(\kappa Q^2)^3 + \cdots + \tilde{d}_n(\kappa) a(\kappa Q^2)^{n+1} + \ldots, \tag{2.14}$$

where we must stress again that although the observable $d(Q^2)$ is renormalisation scheme independent, the quantity in Eq. (2.14) is not, remembering that $\kappa \equiv \mu^2/Q^2$ is the renormalisation scale parameter. For this quantity we can define a Borel transform akin to that in Eq. (2.2) by replacing the coefficients there as $d_n(\kappa) \mapsto \tilde{d}_n(\kappa)$:

$$\mathcal{B}[\tilde{d}](u;\kappa) \equiv 1 + \frac{\tilde{d}_1(\kappa)}{1!\beta_0} u + \frac{\tilde{d}_2(\kappa)}{2!\beta_0^2} u^2 + \cdots + \frac{\tilde{d}_n(\kappa)}{n!\beta_0^n} u^n + \ldots \tag{2.15}$$

Part of the reason we constructed the rewritten expansion series (Eq. (2.14)) coefficients and the rewritten Borel transform (Eq. (2.15)) is because these turn out to have a much simpler κ-dependence than the originals ($d_n(\kappa)$ and $\mathcal{B}[d](u;\kappa)$), which we will now proceed to derive. Noting that $d\ln\mu^2 = d\ln\kappa$, we recall the definition of the logarithmic derivatives $\tilde{a}_n(\kappa Q^2)$ in Eq. (2.4), from where it is clear that

$$\frac{d}{d\ln\kappa} \tilde{a}_n(\kappa Q^2) = (-\beta_0) n \tilde{a}_{n+1}(\kappa Q^2). \tag{2.16}$$

With this, we can now apply $d/d\ln\kappa$ to $d(Q^2)_{\log}$ in Eq. (2.10), which gives

$$\frac{d}{d\ln\kappa} d(Q^2) = \sum_{n=1}^{\infty} \tilde{a}_{n+1}(\kappa Q^2) \left((-\beta_0) n \tilde{d}_{n-1}(\kappa) + \frac{d}{d\ln\kappa} \tilde{d}_n(\kappa) \right). \tag{2.17}$$

But, remembering that $d(Q^2)$ must be μ^2-independent, this last equation must

be identically equal to zero, which means each coefficient at $\tilde{a}_{n+1}(\kappa Q^2)$ must also be zero, hence it clearly follows that

$$\frac{d}{d\ln\kappa}\tilde{d}_0(\kappa) = 0,$$

$$\frac{d}{d\ln\kappa}\tilde{d}_n(\kappa) = n\beta_0\tilde{d}_{n-1}(\kappa) \quad (n \geq 1). \tag{2.18}$$

Note that each of these expressions can be integrated: from the first it follows that the result $\tilde{d}_0(\kappa) = 1$ is valid for any κ and thus for any renormalisation scale, while from Eq. (2.18) we get

$$\tilde{d}_n(\kappa) = \tilde{d}_n(\kappa = 1) + \sum_{k=1}^{n} \binom{n}{k} (\beta_0 \ln\kappa)^k \tilde{d}_{n-k}(\kappa = 1) \quad (n \geq 1). \tag{2.19}$$

For the κ-dependence of the Borel transform of $\tilde{d}(Q^2)$, we now take the derivative $d/d\ln\kappa$ of $\mathcal{B}[\tilde{d}](u;\kappa)$ in Eq. (2.15) considering the relation in Eq. (2.18), which results in

$$\frac{d}{\ln\kappa}\mathcal{B}[\tilde{d}](u;\kappa) = u\mathcal{B}[\tilde{d}](u;\kappa) \tag{2.20}$$

$$\implies \mathcal{B}[\tilde{d}](u;\kappa) = \kappa^u \mathcal{B}[\tilde{d}](u;\kappa = 1). \tag{2.21}$$

As this last equation shows, the Borel transform of $\tilde{d}(Q^2)$ has an especially simple κ-dependence which can be simply included by a factor in front of a version evaluated with $\kappa = 1$, which means that it is of the one-loop *type* (large-β_0 where $\beta_j \mapsto 0$ for $j = 1, 2, \dots$) while not being in the one-loop approximation at all; the dependence is exact. This is in contrast to the κ-dependence of the original quantities $d_n(\kappa)$ and $\mathcal{B}[d](u;\kappa)$, that have this kind of simple structure only in the one-loop approximation [16, 34]. This is a clear advantage of the method [8] we're using, since it also implies that the renormalon structure of $\mathcal{B}[\tilde{d}](u;\kappa)$ must be very close to that of the large-β_0 structure of $\mathcal{B}[d](u)$, which is known (see Refs. [16, 34]), and thus we can make an *ansatz* for it to generate a valid resummation in a simpler manner than what the unmodified Borel transform allows.

In light of this last fact, let us briefly discuss what we know about the expected renormalon structures of the Borel transforms of spacelike observables.

2.2 Renormalon Structure of Spacelike Observables

As we mentioned in the last section, all the κ-dependence considerations suggest that the Borel transform $\mathcal{B}[\tilde{d}](u;\kappa)$ has a renormalon structure of the one-loop, large β_0 type similar to that of $\mathcal{B}[d](u)$. From Refs. [16, 34] we know that the theoretically expected renormalon structure of $\mathcal{B}[d](u)$ is

$$\mathcal{B}[d](u) \propto \frac{1}{(p-u)^{\xi+p\beta_1/\beta_0^2}}(1+\mathcal{O}(p-u)), \quad \frac{1}{(p+u)^{\xi-p\beta_1/\beta_0^2}}(1+\mathcal{O}(p+u)), \tag{2.22}$$

where p is a positive integer and ξ can have any positive value (not necessarily integer) to be fixed according to the observable we evaluate. These structures correspond, respectively, to the beyond-large-β_0 type IR renormalon at $u=p$ and to the beyond-large-β_0 UV renormalon at $u=-p$. It can be shown numerically (see Refs. [8, 35]) that these imply that the corresponding renormalons in $\mathcal{B}[\tilde{d}](u;\kappa)$ have a structure:

$$\mathcal{B}[\tilde{d}](u) \propto \frac{1}{(p-u)^{\xi}}(1+\mathcal{O}(p-u)), \quad \frac{1}{(p+u)^{\xi}}(1+\mathcal{O}(p-u)), \tag{2.23}$$

which happen to be precisely the structures in Eq. (2.22) in the limit $\beta_0 \to \infty$. These type of terms that appear in $\mathcal{B}[\tilde{d}](u;\kappa)$ will generate different coefficients $\tilde{d}_n$ depending on the exact structure of each observable we want to evaluate, which we will use to generate appropriate, possibly even physically motivated, *ansätze* that generate the expected and known values of the coefficients by adjusting the weight of each term accordingly.

We note that if we take one of the possibilities from Eq. (2.22), e.g the case $u=p$, and use it in Eq. (2.3) we can obtain the Q^2-dependence of renormalon-induced ambiguity in the integration

$$\delta d(Q^2)_{p,\xi} \sim \frac{1}{\beta_0}\mathrm{Im}\int_{0+i\epsilon}^{\infty+i\epsilon} du\ \exp\left(-\frac{u}{\beta_0 a(Q^2)}\right)\frac{1}{(p-u)^{\xi+pc_1/\beta_0}}, \tag{2.24}$$

$$\sim \frac{1}{(Q^2)^p}a(Q^2)^{1-\xi}\left(1+\mathcal{O}(a)\right), \tag{2.25}$$

with which we can inform our choice of renormalon structure in the $\mathcal{B}[\tilde{d}](u;\kappa)$

ansatz for our observable so that it is related to the structure of the OPE. Namely, the Q^2-dependence in Eq. (2.25) should reasonably be the same as the Q^2-dependence of the $2p$-dimensional ($D = 2p$) term of the OPE for the observable $d(Q^2)$.

With this and all that was developed in the previous section, we have what we need to continue with the method, which calls now for the use of M. Neubert's construction [36, 37] to generate the characteristic function $F_d(t)$ of the resummation of $d(Q^2)$. Neubert constructed these characteristic functions in the large-β_0 approximation in pQCD, but Cvetič's method actually follows this approach for *ansätze* of $\mathcal{B}[\tilde{d}](u;\kappa)$ and thus extends the method beyond large-β_0.

2.3 Obtaining the Characteristic Function and Resummation

Now, as is required in the method we follow [8] in this work, we must now use an approach akin to Neubert's [36, 37], with which we can perform the resummation of $d(Q^2)$ through the use of an *ansatz* for $\mathcal{B}[\tilde{d}](u;\kappa)$ generated according to the renormalon structure explained in the previous section. This last formulation is what is novel about Cvetič's use of Neubert's procedure, and it starts with the fact that the resummation of $d(Q^2)$ can be written in the form

$$d(Q^2)_{\text{res}} = \int_0^\infty \frac{dt}{t} F_d(t) a(tQ^2), \tag{2.26}$$

where $a(Q^2)$ is the QCD running coupling (at any loop order) and $F_d(t)$ is the so called characteristic function of $d(Q^2)$, the leading-twist, canonical part of an observable. Very importantly, it turns out that $F_d(t)$ is directly related to the modified Borel transform $\mathcal{B}[\tilde{d}](u;\kappa)$ from Eq. (2.15). We construct the characteristic function by first performing a Taylor expansion of $a(tQ^2)$ in Eq. (2.26) around $\mu^2 = \kappa Q^2$

$$a(tQ^2) = a(\kappa Q^2) + (-\beta_0)\ln(t/\kappa)\tilde{a}_2(\kappa Q^2) + \cdots + (-\beta_0)^n \ln^n(t/\kappa)\tilde{a}_{n+1}(\kappa Q^2) + \ldots \tag{2.27}$$

Given that in the expansion of $d(Q^2)$ in logarithmic derivatives $\tilde{a}_{n+1}$ from Eq. (2.10) the expansion coefficients are $\tilde{d}_n(\kappa)$, we exchange integration and summation with which we conclude that $F_d(t)$ must be a function that satisfies the relations

$$\tilde{d}_n(\kappa) = (-\beta_0)^n \int_0^{+\infty} \frac{dt}{t} F_d(t) \ln^n \frac{t}{\kappa}, \quad (n = 0, 1, 2, \dots). \tag{2.28}$$

It is important to note that this expression can be used to check a priori (i.e. after the construction of F_d) the consistency of the method applied, by making sure the characteristic function based on our modified Borel transform *ansatz* reproduces the known $\tilde{d}_n$ coefficients. We can relate the conditions in Eq. (2.28) to $\mathcal{B}[\tilde{d}](u;\kappa)$ by multiplying the factor $u^n/(n!\beta_0^n)$ conveniently and summing over n, which means that

$$\begin{aligned} \mathcal{B}[\tilde{d}](u;\kappa) &= \int_0^{\infty} \frac{dt}{t} F_d(t) \sum_{n=0}^{\infty} \frac{1}{n!} \left(-u \ln\left(t/\kappa\right)\right)^n \\ \implies \mathcal{B}[\tilde{d}](u;\kappa) &= \int_0^{\infty} \frac{dt}{t} F_d(t) t^{-u} \kappa^u. \end{aligned} \tag{2.29}$$

But taking into account the relation in Eq. (2.21), the common factor κ^u is cancelled out on both sides and thus we obtain the completely κ-independent relation

$$\mathcal{B}[\tilde{d}](u, \kappa = 1) = \mathcal{B}[\tilde{d}](u) = \int_0^{\infty} \frac{dt}{t} F_d(t) t^{-u}, \tag{2.30}$$

the structure of which very importantly, centrally, and conveniently to Cvetič's method leads us to conclude that the modified Borel transform $\mathcal{B}[\tilde{d}](u)$ is the Mellin transform of the characteristic function $F_d(t)$. In turn, this means that the characteristic function of observable $d(Q^2)$ turns out to be the inverse Mellin transform of $\mathcal{B}[\tilde{d}](u)$ κ-independently:

$$F_d(t) = \frac{1}{2\pi i} \int_{u_0 - i\infty}^{u_0 + i\infty} du \; \mathcal{B}[\tilde{d}](u) t^u. \tag{2.31}$$

Here, u_0 is any value close to zero where the Mellin transform exists. Hence we have satisfactorily constructed the resummation of $d(Q^2)$ from Eq. (2.26), based only on the knowledge of the expansion coefficients $\tilde{d}_n(\kappa)$ at a given value of κ and the relations previously derived. However, very importantly, we note that the characteristic function and resummation this way obtained are κ-independent, as is expected of the original observable.

In the next chapter, we will apply the method outlined in this chapter specifically to the Bjorken Sum Rule (BSR).

Chapter 3

Applying the Method to the BSR

Using Cvetič's method outlined in Chapter 2, we now carry on to the main part of this thesis: generating the resummation for the canonical OPE part of the prototypical QCD sum rule, the Bjorken Sum Rule, which we described in detail earlier in Section 1.4. First though, we note that in our work we used a modified version of the OPE from that of Eq. (1.8), which includes an extra term to consider the possible nondecoupling of the charm quark as a correction instead of decoupling it as an infinitely heavy favour

$$\overline{\Gamma}_1^{p-n,\mathrm{OPE}}(Q^2) = \left|\frac{g_A}{g_V}\right|\frac{1}{6}(1 - d(Q^2) - \delta d(Q^2)_{m_c}) + \sum_{i=2}^{\infty}\frac{\mu_{2i}(Q^2)}{Q^{2i-2}}, \tag{3.1}$$

where $|g_A/g_V| = 1.2754$ is still the ratio of the nucleon axial charge, and $d(Q^2)$ is still the canonical dimension zero QCD part where we take $n_f = 3$ with all the characteristics mentioned in Section 1.4. The term $\delta d(Q^2)_{m_c}$ is the correction to introduce the nondecoupling of the charm quark mass. This term is known from previous literature [38], and can be written as

$$\delta d(Q^2)_{m_c} = \frac{1}{6}\left(\ln\left(\frac{Q^2}{m_c^2}\right) - 2C_{\mathrm{pBJ}}^{\mathrm{mass.},(2)}\left(\frac{Q^2}{m_c^2}\right)\right)a(Q^2)^2 + \mathcal{O}(a^3), \tag{3.2}$$

where $m_c \approx 1.67$ GeV [39] is the pole mass of the charm quark, and $C_{\mathrm{pBJ}}^{\mathrm{mass.},(2)}$ is derived explicitly in [38]. More details of this term's inclusion and meaning can be found in Appendix A of our recent work [10], but this part is not very central to this

thesis.

3.1 Generation of the *ansatz* for $\mathcal{B}[\tilde{d}](u)$

We start by generating a reasonable, physically motivated, *ansatz* for $\mathcal{B}[\tilde{d}](u;\kappa)$. Due to the known large-β_0 structure of the unmodified Borel transform $\mathcal{B}[d](u;\kappa)$ [16, 34] of the expansion of the observable, we can use this to inform the structure of our *ansatz* for the modified transform as explained at the end of Section 2.1 due to the expressions there derived. This, in addition to the fact that their renormalon structures must be similar as argued in Section 2.2, motivates us to select an *ansatz* at $\kappa = 1$:

$$\mathcal{B}[\tilde{d}](u) = \exp\left(\tilde{K}u\right)\pi\left[\tilde{d}_1^{\mathrm{IR}}\frac{1}{(1-u)^{\xi}} + \tilde{d}_2^{\mathrm{IR}}\frac{1}{(2-u)} + \tilde{d}_1^{\mathrm{UV}}\frac{1}{(1+u)} + \tilde{d}_2^{\mathrm{UV}}\frac{1}{(2+u)}\right] \tag{3.3}$$

Here, $\xi = 1 - k_1 = 49/81$, where $k_1 = 32/81$ is the known exact anomalous dimension of the $D = 2$ OPE term as mentioned in Section 1.4 (cf. also Eq.(2.25)). We note that $\xi \neq 1$ because we know the exact anomalous dimension of the $D = 2$ term, but for the higher terms this is not the case. For these we know only the large-β_0 value of the anomalous dimension, which is zero, and thus all the other terms of our *ansatz* have an exponent equal to one since we don't have more information to modify it.

This proposed *ansatz* of Eq. (3.3) generates, via the expansion of Eq. (2.15), the coefficients $\tilde{d}_n(\kappa = 1)$. We have only five parameters: the rescaling parameter $\tilde{K}$, and the renormalon residues $\tilde{d}_1^{\mathrm{IR}}, \tilde{d}_2^{\mathrm{IR}}, \tilde{d}_1^{\mathrm{UV}}, \tilde{d}_2^{\mathrm{UV}}$. The five parameters are determined quite simply by solving the system of equations thus established, due to the knowledge of the first few coefficients d_n (and therefore $\tilde{d}_n$ too), i.e. for $n = 0, 1, 2, 3, 4$ previously established in the first Chapter. The resulting values are here presented in Table 3.1 in the five-loop $\overline{\mathrm{MS}}$ scheme as an example, since this is one of the schemes we used in our evaluation in Refs. [9, 10].

Due to the relation found earlier in Eq. (2.21), we can modify the proposed Borel transform in Eq. (3.3) quite simply to that where $\kappa \neq 1$, which according to that

Table 3.1: The values of $\widetilde{K}$ and of the renormalon residues $\widetilde{d}_j^{\mathrm{X}}$ (X=IR,UV) for the five-parameter *ansatz* Eq. (3.3) in the 5-loop $\overline{\mathrm{MS}}$ scheme, where the d_4 taken is such that it corresponds to the 5-loop $\overline{\mathrm{MS}}$ value $d_4^{\overline{\mathrm{MS}}} = 1557.43$ (as predicted by ECH), as obtained by solving the system of equations established with Eq. (2.15).

scheme	$\widetilde{K}$	$\widetilde{d}_1^{\mathrm{IR}}$	$\widetilde{d}_2^{\mathrm{IR}}$	$\widetilde{d}_1^{\mathrm{UV}}$	$\widetilde{d}_2^{\mathrm{UV}}$
$\overline{\mathrm{MS}}$ (5-loop)	-1.82336	7.81560	-14.8199	-0.0413348	-0.0920349

equation results in

$$\mathcal{B}[\tilde{d}](u) = \exp\Big((\ln\kappa + \tilde{K})u\Big)\,\pi\left[\tilde{d}_1^{\mathrm{IR}}\frac{1}{(1-u)^{\xi}} + \tilde{d}_2^{\mathrm{IR}}\frac{1}{(2-u)} + \tilde{d}_1^{\mathrm{UV}}\frac{1}{(1+u)} + \tilde{d}_2^{\mathrm{UV}}\frac{1}{(2+u)}\right]. \tag{3.4}$$

It turns out that solving the same system of equation as with Eq. (3.3) and $\tilde{d}_n(\kappa = 1)$ but with Eq. (3.4) and $\tilde{d}_n(\kappa)$ returns the exact same results por the five parameters as in the first case, those of Table 3.1. This shows the consistency of the chosen approach and solidifies the conclusions of Eqs. (2.21) and (2.30), because it means that we can use our first $\mathcal{B}[\tilde{d}](u)$ *ansatz* Eq. (3.3) with no loss of generality for our resummation due to its κ-independence. For this goal, in the next section we will look for the characteristic function of the resummation $d(Q^2)_{\mathrm{res}}$ we wish to perform but we start with Eq. (3.3) set in the case where $\tilde{K} = 0$, since $\tilde{K}$ is only a rescaling of the variable and thus can be included later.

3.2 Full Computation of the Characteristic Function

We will now proceed to use the *ansatz* to compute the characteristic function $G_d(t)$ (i.e. the version with $\tilde{K} \mapsto 0$, for the reasons explained earlier) we need for the resummation $d(Q^2)_{\mathrm{res}}$. We'll not consider at first the contribution of the $e^{\tilde{K}u}$ factor, because we'll include it in a trivial manner later. When $\mathcal{B}[\tilde{d}](u)$ fulfils convergence conditions, its inverse Mellin transform (wherever it exists) gives us this quantity for a value of $u_0 \in \,]-1, 1[$, specifically one close to zero, thus:

$$G_d(t) = \frac{1}{2\pi i}\int_{u_0-i\infty}^{u_0+i\infty} du \;\; \mathcal{B}[\tilde{d}](u)\Big|_{\tilde{K}\mapsto 0} t^u \tag{3.5}$$

$$-1 < u_0 < +1 \implies G_d(t) = \frac{t}{2\pi}\int_{-\infty}^{+\infty} dz \;\; \mathcal{B}[\tilde{d}](u = 1 - iz)\Big|_{\tilde{K}\mapsto 0} e^{-iz\ln(t)}$$

$$G_d(t) = \frac{t}{2}\int_{-\infty}^{+\infty} dz \left(\frac{\tilde{d}_1^{\text{IR}}}{(iz)^{\xi}} + \frac{\tilde{d}_2^{\text{IR}}}{(1+iz)} + \frac{\tilde{d}_1^{\text{UV}}}{(2-iz)} + \frac{\tilde{d}_2^{\text{UV}}}{(3-iz)}\right) e^{-iz\ln(t)}. \tag{3.6}$$

Where the residues $\tilde{d}_1^{\text{IR}}, \tilde{d}_2^{\text{IR}}, \tilde{d}_1^{\text{UV}}, \tilde{d}_2^{\text{UV}}$ are, for example, those that appear in Table 4.1 and $\xi = 49/81$ is the anomalous dimension of the $D = 2$ OPE term of the BSR. We can separate the terms in the integral, so then $G_d(t)$ is actually:

$$\begin{aligned} G_d(t) = \frac{t}{2}\Bigg[&\tilde{d}_1^{\text{IR}}\int_{-\infty}^{+\infty} dz \frac{e^{-iz\ln(t)}}{(iz)^{\xi}} + \tilde{d}_2^{\text{IR}}\int_{-\infty}^{+\infty} dz \frac{e^{-iz\ln(t)}}{(1+iz)} \\ &+\tilde{d}_1^{\text{UV}}\int_{-\infty}^{+\infty} dz \frac{e^{-iz\ln(t)}}{(2-iz)} + \tilde{d}_2^{\text{UV}}\int_{-\infty}^{+\infty} dz \frac{e^{-iz\ln(t)}}{(3-iz)}\Bigg] \end{aligned} \tag{3.7}$$

Each of these terms can then be solved separately with careful integration. For the $\tilde{d}_2^{\text{IR}}$ term

$$\mathcal{J}_{(\text{IR},2)}(t) = \int_{-\infty}^{+\infty} dz \frac{e^{-iz\ln(t)}}{(1+iz)}, \tag{3.8}$$

we have a simple pole at $z = i$, so we use contour integration along a path that contains the pole, when $0 < t < 1$, such as:

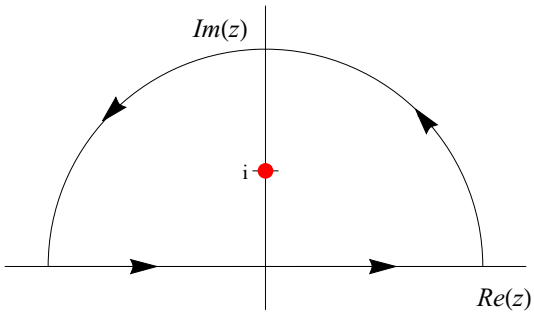

Figure 3.1: Closed contour of integration in the complex plane for the integrand in Eq. (3.8), when $0 < t < 1$ ($\ln t < 0$). Note the simple pole at $z = i$, which is encircled by our contour and thus allows us to use Cauchy's residue theorem. The upper semicircle, of radius R, has a null contribution when $R \to \infty$ (see text).

We consider here only the upper semicircle (as seen in Fig. 3.1), i.e. the case when $0 < t < 1$ ($\ln t < 0$), because the contour with a lower semicircle (i.e. the case when $t > 1$) contains no singularity so its contribution is null. Since this is a simple pole, we can use Cauchy's residue theorem to solve the original integral through the contour version quite simply by integrating

$$\int_{\mathrm{C}} dz \frac{e^{-iz\ln(t)}}{(1+iz)} \tag{3.9}$$

$$= 2\pi i \ \mathrm{Res}_{z=i}\left(\frac{e^{-iz\ln(t)}}{(1+iz)}\right) = 2\pi i \lim_{z\to i}\left((z-i)\,\frac{e^{-iz\ln(t)}}{(1+iz)}\right) = 2\pi i(-it) = 2\pi t, \tag{3.10}$$

where we can decompose the contour integral in the two parts of the contour (straight and arc)

$$\int_{\mathrm{C}} dz \frac{e^{-iz\ln(t)}}{(1+iz)} = \int_{\mathrm{arc}} dz \frac{e^{-iz\ln(t)}}{(1+iz)} + \int_{-R}^{R} dz \frac{e^{-iz\ln(t)}}{(1+iz)} = 2\pi t. \tag{3.11}$$

We know the arc term to be bounded in the following way using Jordan's lemma:

$$\left|\int_{\mathrm{arc}} dz \frac{e^{-iz\ln(t)}}{(1+iz)}\right| \leq \frac{\pi}{|\ln(t)|} \cdot \max_{\theta\in[0,\pi]}\left|\frac{1}{(1+iRe^{i\theta})}\right|. \tag{3.12}$$

Noting however that for large $|R|$

$$\left|\frac{1}{(1+iRe^{i\theta})}\right| \approx \left|\frac{1}{R}\right|, \tag{3.13}$$

we can actually write the bound for the arc integral as

$$\left|\int_{\text{arc}} dz \frac{e^{-iz\ln(t)}}{(1+iz)}\right| \leq \frac{\pi}{|\ln(t)|} \cdot \left|\frac{1}{R}\right|,$$

from where it then follows quite naturally that for $R \to \infty$:

$$\int_{\text{C}} dz \frac{e^{-iz\ln(t)}}{(1+iz)} = \cancelto{0}{\int_{\text{arc}} dz \frac{e^{-iz\ln(t)}}{(1+iz)}} + \int_{-\infty}^{+\infty} dz \frac{e^{-iz\ln(t)}}{(1+iz)} = 2\pi t \tag{3.14}$$

$$\implies \mathcal{J}_{(\text{IR},2)}(t) = \int_{-\infty}^{+\infty} dz \frac{e^{-iz\ln(t)}}{(1+iz)} = 2\pi t, \tag{3.15}$$

which is therefore the value of the $\tilde{d}_2^{\text{IR}}$ term that enters into the characteristic function $G_d(t)$ that we were looking for. As mentioned before, when $t > 1$ ($\ln t > 0$) the contour is closed by a lower semicircle that encloses no singularity, and thus when applying Jordan's lemma to that part $\mathcal{J}_{(\text{IR},2)}(t) = 0$.

Similarly, for the $\tilde{d}_1^{\text{UV}}$ term

$$\mathcal{J}_{(\text{UV},1)}(t) = \int_{-\infty}^{+\infty} dz \frac{e^{-iz\ln(t)}}{(2-iz)}, \tag{3.16}$$

once again we have a simple pole, but this time at $z = -2i$, so we take a path such as:

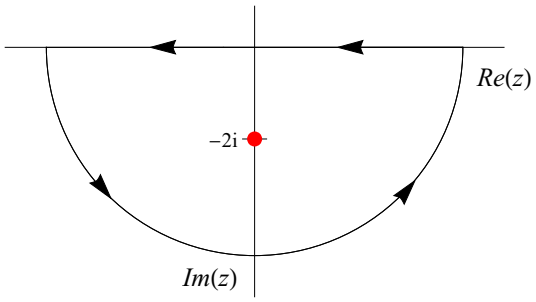

Figure 3.2: Closed contour of integration in the complex plane for the integrand in Eq. (3.16), when $t > 1$ ($\ln t > 0$). Note the simple pole at $z = -2i$, which is encircled by the contour and thus allows the use of Cauchy's residue theorem. The lower semicircle, of radius R, has null contribution when $R \to \infty$ (see text).

Thus we now consider only the lower semicircle (as can be seen in Fig. 3.2), i.e. the case when $t > 1$ ($\ln t > 0$), because the contour with an upper semicircle (i.e. the case $0 < t < 1$) is the one that contains no singularity and thus gives null contribution. Once again we use Cauchy's residue theorem to solve the integral through the contour version by integrating

$$\int_{\mathrm{C}} dz \frac{e^{-iz\ln(t)}}{(2-iz)} \tag{3.17}$$

$$= 2\pi i \ \mathrm{Res}_{z=-2i}\left(\frac{e^{-iz\ln(t)}}{(2-iz)}\right) = 2\pi i \lim_{z\to -2i}\left((z+2i)\frac{e^{-iz\ln(t)}}{(2-iz)}\right) = 2\pi i\left(\frac{i}{t^2}\right) = -\frac{2\pi}{t^2}, \tag{3.18}$$

where we can once again decompose the contour integral

$$\int_{\mathrm{C}} dz \frac{e^{-iz\ln(t)}}{(2-iz)} = \int_{\mathrm{arc}} dz \frac{e^{-iz\ln(t)}}{(2-iz)} + \int_{R}^{-R} dz \frac{e^{-iz\ln(t)}}{(2-iz)} = -\frac{2\pi}{t^2}. \tag{3.19}$$

The arc term is then bounded in a similar way as in the previous case through Jordan's lemma

$$\left|\int_{\mathrm{arc}} dz \frac{e^{-iz\ln(t)}}{(2-iz)}\right| \leq \frac{\pi}{\ln(t)} \cdot \max_{\theta\in[\pi,2\pi]}\left|\frac{1}{(2-iRe^{i\theta})}\right|. \tag{3.20}$$

Just as in the previous case, for large $|R|$

$$\left|\frac{1}{(2-iRe^{i\theta})}\right| \approx \left|\frac{1}{R}\right|, \tag{3.21}$$

hence we write the bound for the arc integral as

$$\left|\int_{\text{arc}} dz \frac{e^{-iz\ln(t)}}{(2-iz)}\right| \leq \frac{\pi}{\ln(t)} \cdot \left|\frac{1}{R}\right|,$$

from where it is easy to see that in the limit $R \to \infty$

$$\int_{\text{C}} dz \frac{e^{-iz\ln(t)}}{(2-iz)} = \cancelto{0}{\int_{\text{arc}} dz \frac{e^{-iz\ln(t)}}{(2-iz)}} + \int_{\infty}^{-\infty} dz \frac{e^{-iz\ln(t)}}{(2-iz)} = -\frac{2\pi}{t^2} \tag{3.22}$$

$$\implies \mathcal{J}_{(\text{UV},1)}(t) = \int_{-\infty}^{\infty} dz \frac{e^{-iz\ln(t)}}{(2-iz)} = \frac{2\pi}{t^2}, \tag{3.23}$$

which is therefore the value of the $\tilde{d}_1^{\text{UV}}$ integral we wanted for $G_d(t)$. As mentioned before, in this case when $0 < t < 1$ the contour is closed from above and thus by Jordan's lemma we get $\mathcal{J}_{(\text{UV},1)}(t) = 0$ since such a contour would contain no sengularity.

In much the same way as the two previous cases, for the $\tilde{d}_2^{\text{UV}}$ term

$$\mathcal{J}_{(\text{UV},2)}(t) = \int_{-\infty}^{\infty} dz \frac{e^{-iz\ln(t)}}{(3-iz)}, \tag{3.24}$$

where we again have a simple pole, this time at $z = -3i$, so the path we take is:

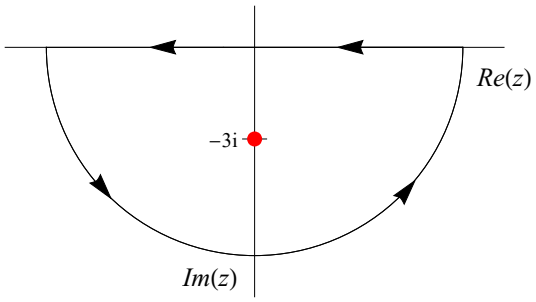

Figure 3.3: Closed contour of integration in the complex plane for the integrand in Eq. (3.24), when $t > 1$ ($\ln t > 0$). Note the simple pole at $z = -3i$, which is encircled by the contour and thus allows the use of Cauchy's residue theorem. The lower arc, of radius R, contributes zero when $R \to \infty$ (see text).

We take again only the lower semicircle (as can be seen in Fig. 3.3), the case when $t > 1$ ($\ln t > 0$). Then, we can use Cauchy's residue theorem to solve the integral through the contour version

$$\int_C dz \frac{e^{-iz\ln(t)}}{(3-iz)} \tag{3.25}$$

$$2\pi i \ \mathrm{Res}_{z=-3i}\left(\frac{e^{-iz\ln(t)}}{3-iz}\right) = 2\pi i \lim_{z\to -3i}\left((z+3i)\frac{e^{-iz\ln(t)}}{(3-iz)}\right) = 2\pi i\left(\frac{i}{t^3}\right) = -\frac{2\pi}{t^3}, \tag{3.26}$$

where this contour integral can be decomposed as

$$\int_{\mathrm{C}} dz \frac{e^{-iz\ln(t)}}{(3-iz)} = \int_{\mathrm{arc}} dz \frac{e^{-iz\ln(t)}}{(3-iz)} + \int_R^{-R} dz \frac{e^{-iz\ln(t)}}{(3-iz)} = -\frac{2\pi}{t^3}. \tag{3.27}$$

The arc term is bounded according to Jordan's lemma

$$\left|\int_{\mathrm{arc}} dz \frac{e^{-iz\ln(t)}}{(3-iz)}\right| \leq \frac{\pi}{\ln(t)} \cdot \max_{\theta\in[\pi,2\pi]}\left|\frac{1}{(3-iRe^{i\theta})}\right|. \tag{3.28}$$

In particular, for large $|R|$ we have

$$\left|\frac{1}{(3-iRe^{i\theta})}\right| \approx \left|\frac{1}{R}\right|, \tag{3.29}$$

hence the bound for the arc integral is

$$\left|\int_{\text{arc}} dz \frac{e^{-iz\ln(t)}}{(3-iz)}\right| \leq \frac{\pi}{\ln(t)} \cdot \left|\frac{1}{R}\right|,$$

from where it follows that in the limit $R \to \infty$

$$\int_{\text{C}} dz \frac{e^{-iz\ln(t)}}{(3-iz)} = \cancelto{0}{\int_{\text{arc}} dz \frac{e^{-iz\ln(t)}}{(3-iz)}} + \int_{\infty}^{-\infty} dz \frac{e^{-iz\ln(t)}}{(3-iz)} = -\frac{2\pi}{t^3} \tag{3.30}$$

$$\implies \mathcal{J}_{(\text{UV},2)}(t) = \int_{-\infty}^{\infty} dz \frac{e^{-iz\ln(t)}}{(3-iz)} = \frac{2\pi}{t^3}, \tag{3.31}$$

which is therefore the value of the $\tilde{d}_2^{\text{UV}}$ integral we wanted for $G_d(t)$. As mentioned earlier, for the case when $0 < t < 1$, the contour is closed from above and and through Jordan's lemma we get for that part $\mathcal{J}_{(\text{UV},2)}(t) = 0$ since that contour would contain no singularity.

Finally, for the $\tilde{d}_1^{\text{IR}}$ term the procedure is different from the other cases, because we do not have a simple pole. For this term

$$\mathcal{J}_{(\text{IR},1)}(t) = \int_{-\infty}^{+\infty} dz \frac{e^{-iz\ln(t)}}{(iz)^{\xi}}, \tag{3.32}$$

where $0 < \xi < 1$, we can see that we have not only a pole but also a cut in the positive imaginary semiaxis ($iz \leq 0$), so in this case we use contour integration with a path that *does not* contain the cut such as:

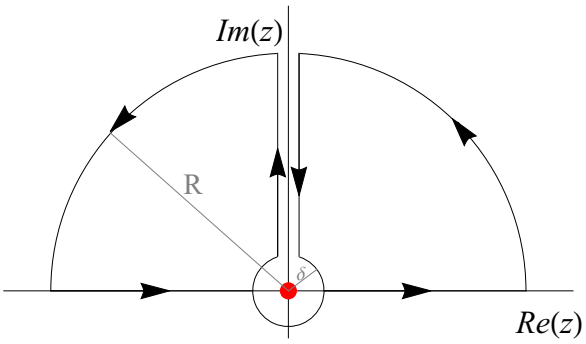

Figure 3.4: Closed contour of integration in the complex plane for the integrand in Eq. (3.32), when $0 < t < 1$ ($\ln t < 0$). Note that the contour does not enclose the pole at $z = 0$ nor the whole positive imaginary semiaxis. We have vertical lines of integration where $z = i(s) \pm \epsilon$, for $\delta < s < R$. For limits we will use $R \to \infty$ and $0 < \epsilon \ll \delta \to +0$.

It is clear from Figs. 3.4 that the path we need passes twice through the lower arc of the circle around the pole, which can be seen separately in Fig. 3.5. For our evaluation we can take a different variable $\delta < s < R$, with which in the vertical part of the path we then have $z = i(s) \pm \epsilon$ where $0 < \epsilon \ll \delta$. To evaluate our integrals we will eventually take the limits $\delta \to +0$ and $R \to \infty$.

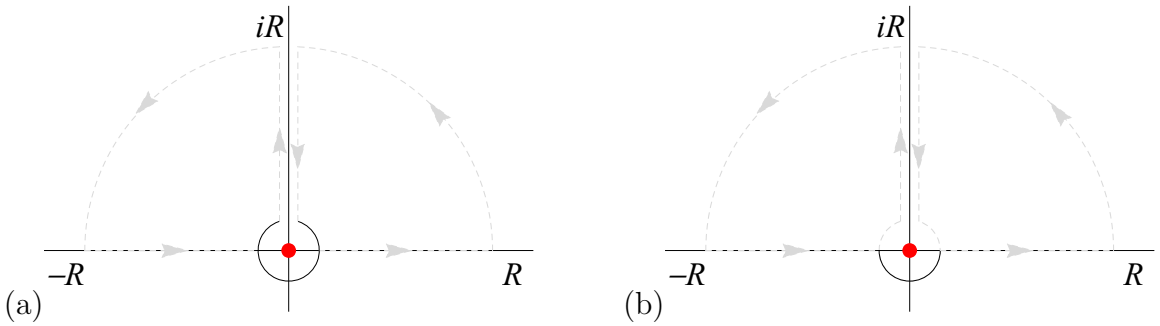

Figure 3.5: Sections of the contour from Fig. 3.4 that pass around the pole at $z = 0$, both of which give no contribution to the full integral as is shown in the text. (a) Circular portion of the contour around the pole, traced clockwise. (b) Semicircular portion of the contour around the pole, traced counterclockwise.

First, we can prove that the circular (and in the same way the semicircular) part around the pole from Fig. 3.5 does not contribute

$$\mathcal{J}_{\text{circ}}(t) = \int_{\text{circ}} dz \frac{e^{-iz\ln(t)}}{(iz)^{\xi}}, \tag{3.33}$$

by first noting that

$$z = \delta e^{i\theta} = \delta\cos\theta + i\delta\sin\theta \implies dz = \delta e^{i\theta} i d\theta, \tag{3.34}$$

and that $(i)^{-\xi} = e^{-i\frac{\pi}{2}\xi}$, and also $|z| = \delta$ because of the radius of the circle, we can see that

$$\mathcal{J}_{\text{circ}}(t) = e^{-i\frac{\pi}{2}\xi} \int_{\text{circ}} dz\ z^{-\xi} e^{-iz\ln(t)} \tag{3.35}$$

$$= e^{-i\frac{\pi}{2}\xi} \int_{\text{circ}} d\theta\ i\delta e^{i\theta} \delta^{-\xi} e^{-i\xi\theta} e^{-i(\delta e^{i\theta})\ln(t)}$$

$$= \delta^{(1-\xi)} \left(e^{-i\frac{\pi}{2}\xi}\right) i \int_{\text{circ}} d\theta\ e^{i\theta(1-\xi)} e^{-i(\delta e^{i\theta})\ln(t)}. \tag{3.36}$$

Given that in our case $0 < \xi < 1$, and the integrand is bounded ($|e^{i\theta(1-\xi)}| = 1, \delta \to +0$), when taking the limit we need for our full integration of the term (i.e. $\delta \to +0$) in Eq. (3.36), we see that the factor in front of the integral $\delta^{1-\xi} \to 0$ which means the whole circular (and semicircular) part of the full integral gives a null contribution. We note that the integral in Eq. (3.36) is bounded independently whether the integration is along the circle or the semicircle from Fig. 3.5.

The larger arc of the path also gives a null contribution, on account of it being bounded by Jordan's lemma (when $0 < t < 1$, i.e. $a \equiv -\ln t > 0$)

$$\left| \int_{\text{arc}} \frac{e^{-iz\ln(t)}}{(iz)^{\xi}} \right| \leq \frac{\pi}{\ln(t)} \cdot \max_{\theta\in[0,\pi]} \left| \frac{1}{(iRe^{i\theta})^{\xi}} \right|, \tag{3.37}$$

where we can clearly see that when $R \to \infty$, the limit we shall use later for the integration, the right side goes to zero, thus showing we have no contribution from the larger arc.

Hence, only the horizontal and vertical sections of the path remain to be addressed. Since our path *does not* contain a pole, we know the contributions from those sections must cancel each other according to Cauchy's theorem. Therefore, we gather that the only important contribution for computing $\mathcal{J}_{(\text{IR},1)}(t)$ can be found by simply evaluating that of the vertical sections where $z = i(s) \pm \epsilon$, $\delta < s < R$ (as seen in Fig.

3.4), which we can also separate as

$$\begin{aligned} z_+ &= is + \epsilon \\ z_- &= is - \epsilon, \end{aligned} \tag{3.38}$$

which means that

$$\begin{aligned} dz_+ &= ids \\ dz_- &= ids. \end{aligned} \tag{3.39}$$

Then, given all the conditions we have explained previously and according to Cauchy's theorem, the contribution of the term is given by

$$\begin{aligned} \mathcal{J}_{(\mathrm{IR},1)}(t) &= -\left(\int_R^0 ds \frac{ie^{-iz_+ \ln(t)}}{(iz_+)^\xi} + \int_\delta^R ds \frac{ie^{-iz_- \ln(t)}}{(iz_-)^\xi}\right) \\ &= -\left(\int_\delta^R ds \frac{ie^{-iz_- \ln(t)}}{(iz_-)^\xi} - \int_\delta^R ds \frac{ie^{-iz_+ \ln(t)}}{(iz_+)^\xi}\right) \\ &= -i\int_\delta^R \left(\frac{e^{(s+i\epsilon)\ln(t)}}{(-s-i\epsilon)^\xi} - \frac{e^{(s-i\epsilon)\ln(t)}}{(-s+i\epsilon)^\xi}\right) ds \\ &= -i\int_\delta^R e^{s\ln(t)} \left(\frac{e^{i\epsilon\ln(t)}}{(-s-i\epsilon)^\xi} - \frac{e^{-i\epsilon\ln(t)}}{(-s+i\epsilon)^\xi}\right) ds \\ &= -i\int_\delta^R t^s \left(\frac{t^{i\epsilon}}{(-s-i\epsilon)^\xi} - \frac{t^{-i\epsilon}}{(-s+i\epsilon)^\xi}\right) ds, \end{aligned} \tag{3.40}$$

where the denominators can be rewritten as

$$\begin{aligned} (-s-i\epsilon)^\xi &= \left(\sqrt{s^2+\epsilon^2}\,(\cos\varphi + i\sin\varphi)\right)^\xi \\ (-s+i\epsilon)^\xi &= \left(\sqrt{s^2+\epsilon^2}\,(\cos\varphi + i\sin\varphi)\right)^\xi, \end{aligned} \tag{3.41}$$

therefore, when $e \ll \delta \to +0$, these relations are perfectly fulfilled for $\varphi = -\pi, \pi$ respectively. This and the corresponding selection of φ for each of Eqs. (3.41) can be easily understood when seeing it graphically as in Fig. 3.6.

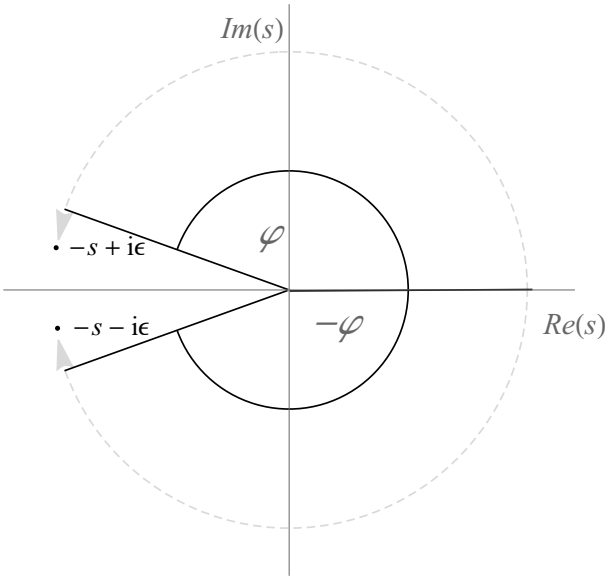

Figure 3.6: Illustrative representation of the selection of the angle φ in Eqs. (3.41), in the complex s-plane. The angles $\varphi, -\varphi$ "approach" the points $(-s+i\epsilon)$ and $(-s-i\epsilon)$ from their respective sides and thus for $\epsilon \to 0$ it is evident that $\varphi = \pi$ is the one we must take for $(-s+i\epsilon)$ and $\varphi = -\pi$ for $(-s-i\epsilon)$.

Now, noting that $\left(\sqrt{s^2+\epsilon^2}\,(\cos\varphi + i\sin\varphi)\right)^{\xi} = (se^{i\varphi})^{\xi}$ in the limit $\epsilon \to +0$, we can make such selection and write

$$\begin{aligned}(-s-i\epsilon)^{\xi} &= \left(se^{-i\pi}\right)^{\xi} \\ (-s+i\epsilon)^{\xi} &= \left(se^{i\pi}\right)^{\xi},\end{aligned} \tag{3.42}$$

with which we can now rewrite $\mathcal{J}_{(\mathrm{IR},1)}(t)$ in Eq. (3.40):

$$\mathcal{J}_{(\mathrm{IR},1)}(t) = -i\int_{\delta}^{R} t^s \left(\frac{t^{i\epsilon}}{(se^{-i\varphi})^{\xi}} - \frac{t^{-i\epsilon}}{(se^{i\varphi})^{\xi}}\right) ds. \tag{3.43}$$

Now, when taking the limits $R \to \infty, \epsilon \to 0$, and afterwards $\delta \to 0$ this gives

$$\begin{aligned}&= -i\int_{0}^{\infty} t^s \left(\frac{1}{(se^{-i\pi})^{\xi}} - \frac{1}{(se^{i\pi})^{\xi}}\right) ds \\ &= -i\int_{0}^{\infty} t^s s^{-\xi}\left(e^{i\pi\xi} - e^{-i\pi\xi}\right) ds,\end{aligned} \tag{3.44}$$

but $\left(e^{i\pi\xi} - e^{-i\pi\xi}\right) = 2i\sin(\xi\pi)$, so this is actually

$$= 2\sin(\xi\pi)\int_0^\infty ds\; t^s s^{-\xi}$$
$$= 2\sin(\xi\pi)\frac{\Gamma(1-\xi)}{\log(1/t)^{1-\xi}}. \tag{3.45}$$

Therefore we conclude that the contribution from the $\tilde{d}_1^{\text{IR}}$ term, when $t < 1$ and $0 < \xi < 1$, is

$$\mathcal{J}_{(\text{IR},1)}(t) = 2\frac{\pi}{\Gamma(\xi)}\frac{1}{(\log(1/t))^{1-\xi}}. \tag{3.46}$$

When $t > 1$, we close the contour from below, but in that case no cuts (and no pole) are enclosed, so we get $\mathcal{J}_{(\text{IR},1)} = 0$ from Jordan's lemma. In that case, the pole at $z = 0$ is avoided as in Fig. 3.5b, or even by a δ-radius semicircle from above; it does not matter in any case because $\delta \to +0$.

With this, we have all we needed to write the full expression for the characteristic function from Eq. (3.7), and so combining Eqs. (3.15), (3.23), (3.31) and (3.46) we get

$$G_d(t) = \left(\tilde{d}_1^{\text{IR}}\frac{\pi}{\Gamma(\xi)}\frac{t}{(\log(1/t))^{1-\xi}} + \tilde{d}_2^{\text{IR}}\pi t^2\right)\Theta(1-t) + \left(\tilde{d}_1^{\text{UV}}\frac{\pi}{t} + \tilde{d}_2^{\text{UV}}\frac{\pi}{t^2}\right)\Theta(t-1), \tag{3.47}$$

3.3 Inclusion of the $e^{\tilde{K}u}$ Factor and Resummation

We will now outline how the $e^{\tilde{K}u}$ factor we "lost" in Eq. (3.5) (because we did not use the full renormalon-motivated *ansatz* from Eq. (3.3)) is to be included to obtain the correct resummation. We want to obtain a characteristic function $F_d(t)$, i.e. the version where $\tilde{K} \neq 0$, for which we will start by taking the direct approach:

$$F_d(t) = \frac{1}{2\pi i}\int_{u_0-i\infty}^{u_0+i\infty} du\; e^{\tilde{K}u}\,\mathcal{B}[\tilde{d}](u)\Big|_{\tilde{K}\mapsto 0}\, t^u \tag{3.48}$$
$$= \frac{t}{2\pi}\int_{-\infty}^{+\infty} dz\; e^{\tilde{K}(1-iz)}\,\mathcal{B}[\tilde{d}](u=1-iz)\Big|_{\tilde{K}\mapsto 0}\, e^{-iz\ln(t)}$$

$$= \frac{te^{\tilde{K}}}{2\pi} \int_{-\infty}^{+\infty} dz \;\; \mathcal{B}[\tilde{d}](u = 1 - iz) \Big|_{\tilde{K} \mapsto 0} e^{-iz \ln(t) - iz\tilde{K}} \tag{3.49}$$

But, since $\tilde{K} = \ln e^{\tilde{K}}$, we can rewrite this as

$$\begin{aligned} F_d(t) &= \frac{te^{\tilde{K}}}{2\pi} \int_{-\infty}^{+\infty} dz \;\; \mathcal{B}[\tilde{d}](u = 1 - iz) \Big|_{\tilde{K} \mapsto 0} e^{-iz(\ln t + \ln e^{\tilde{K}})} \\ &= \frac{te^{\tilde{K}}}{2\pi} \int_{-\infty}^{+\infty} dz \;\; \mathcal{B}[\tilde{d}](u = 1 - iz) \Big|_{\tilde{K} \mapsto 0} e^{-iz \ln(te^{\tilde{K}})} \\ &\implies F_d(t) = G_d(te^{\tilde{K}}). \end{aligned} \tag{3.50}$$

This means that, to include the full Borel transform as required for our resummation, it suffices to take $t' = e^{\tilde{K}} t$ in Eq. (3.5) and following through with the procedure shown earlier, this implies

$$\begin{aligned} \ln t' &= \ln t + \tilde{K} \\ \frac{dt'}{t'} &= \frac{dt}{t}. \end{aligned} \tag{3.51}$$

With this transformation we can then simply use the computation developed in the previous section for $G_d(t)$ for the resummation (Eq. (2.26)) itself

$$d(Q^2)_{\text{res}} = \int_0^\infty \frac{dt}{t} F_d(t) a(tQ^2) = \int_0^\infty \frac{dt'}{t'} G_d(t') a(t' e^{-\tilde{K}} Q^2). \tag{3.52}$$

Then, we just rename our variable $t' \mapsto t$ in the rightmost expression and thus obtain the full resummation using Eq. (3.47) as follows:

$$d(Q^2)_{\text{res}} = \int_0^\infty \frac{dt}{t} G_d(t) a(te^{-\tilde{K}} Q^2) \tag{3.53}$$

$$= \int_0^\infty \frac{dt}{t} t\pi \left(\frac{d_1^{\text{IR}} \, \Theta(1-t)}{\Gamma(\xi) \left(\ln(1/t)\right)^{1-\xi}} + t d_2^{\text{IR}} \, \Theta(1-t) + \frac{d_1^{\text{UV}}}{t^2} \Theta(t-1) + \frac{d_2^{\text{UV}}}{t^3} \Theta(t-1) \right) a(te^{-\tilde{K}} Q^2)$$

$$= \int_0^1 dt \, \pi \left(\frac{d_1^{\text{IR}}}{\Gamma(\xi) \left(\ln(1/t)\right)^{1-\xi}} + t d_2^{\text{IR}} \right) a(te^{-\tilde{K}} Q^2) + \int_1^\infty dt \, \pi \left(\frac{d_1^{\text{UV}}}{t^2} + \frac{d_2^{\text{UV}}}{t^3} \right) a(te^{-\tilde{K}} Q^2). \tag{3.54}$$

Where $\xi = 49/81$ is the anomalous dimension of the $D = 2$ OPE term of the BSR and, in the $\overline{\text{MS}}$ scheme for example, the residues $\tilde{d}_1^{\text{IR}}, \tilde{d}_2^{\text{IR}}, \tilde{d}_1^{\text{UV}}, \tilde{d}_2^{\text{UV}}$ would be those appearing in Table 4.1.

Remembering what was said about the pQCD coupling $a(Q^2)$ in the first Chapter, since it has unphysical Landau singularities at low positive Q^2, these singularities must be avoided in our integration of Eq. (3.53) because it makes the integration ambiguous. This can be accomplished by using a principal value-type regularisation where we slightly deviate from the real axis

$$d(Q^2)_{\text{res}} = \text{Re}\left[\int_0^\infty \frac{dt}{t} G_d(t) a(te^{-\tilde{K}} Q^2 + i\varepsilon)\right]. \tag{3.55}$$

However, as mentioned in the first Chapter, there exist holomorphic variants of QCD (AQCD) which have infrared-safe, holomorphic couplings $\mathcal{A}(Q^2)$ that have no Landau singularities and practically coincide with $a(Q^2)$ at large Q^2. In such cases, no regularisation is needed, and thus the resummation can be directly evaluated as:

$$d(Q^2)_{\text{res,AQCD}} = \int_0^\infty \frac{dt}{t} G_d(t) \mathcal{A}(te^{-\tilde{K}} Q^2). \tag{3.56}$$

This is what we did in Refs. [9, 10] where we made the evaluation of the canonical $d(Q^2)$ part of the BSR with both a pQCD-based resummation as well as an AQCD-based resummation, and also fitted the higher-dimension OPE terms to the experimental data for the BSR up to $D = 4$.

Chapter 4

Resummation Results for the BSR

As mentioned in the previous chapter, we will now briefly discuss some of the results obtained in our recent work [9] (and further expanded upon in [10]) for the evaluation of the polarised Bjorken Sum Rule as outlined in Chapters 2 and 3, and also for the inclusion of the higher-dimension OPE terms up to $D = 4$ through the fitting of our resummation to the available experimental data mentioned in Section 1.4. We start by presenting now the results of the setting of the parameters from the $\mathcal{B}[\tilde{d}](u)$ *ansatz* Eq. (3.3), but now not only in the five-loop $\overline{\text{MS}}$ scheme, in Table 4.1.

Table 4.1: Values for the parameters obtained in our recent work Ref. [9] for various further renormalisation schemes. The values of $\widetilde{K}$ and of the renormalon residues $\widetilde{d}_j^{\text{X}}$ (X=IR,UV) for the five-parameter *ansatz* (3.3) in the (5-loop) $\overline{\text{MS}}$ and in the 'P44' scheme with $c_2 = 9.$ & $c_3 = 20.$, and with $c_2^{\overline{\text{MS}}}(= 4.47106)$ and $c_3^{\overline{\text{MS}}}(= 20.9902)$ (for the schemes 'P44', see Sec. 4.1), when d_4 is taken as that which corresponds to the 5-loop $\overline{\text{MS}}$ value $d_4^{\overline{\text{MS}}} = 1557.43$ (as predicted by ECH). The last line is again for the case of 'P44' scheme with $c_2 = 9.$ & $c_3 = 20.$, but $d_4^{\overline{\text{MS}}} = 1557.43 - 32.84 = 1524.59$.

scheme	$\widetilde{K}$	$\widetilde{d}_1^{\text{IR}}$	$\widetilde{d}_2^{\text{IR}}$	$\widetilde{d}_1^{\text{UV}}$	$\widetilde{d}_2^{\text{UV}}$
$\overline{\text{MS}}$ (5-loop)	-1.82336	7.81560	-14.8199	-0.0413348	-0.0920349
$\overline{\text{MS}}$ (P44)	-1.83223	7.86652	-14.9299	-0.0444416	-0.0776748
$c_2 = 9.$ & $c_3 = 20.$ (P44)	0.450041	0.331813	0.231437	-0.0809782	-0.0964868
$d_4^{\overline{\text{MS}}} = 1524.6$	0.528239	0.276962	0.283465	-0.100381	$\mathcal{O}(10^{-5})$

This shows an interesting behaviour of the parameters when we vary the renor-

malisation scheme, and thus we will now study this variation briefly. For more details omitted here, see Ref. [10].

4.1 Renormalisation scheme variation

First we notice from Table 4.1 that in the $\overline{\rm MS}$ scheme we have the two IR renormalon residues $\widetilde{d}_1^{\rm IR}$ and $\widetilde{d}_2^{\rm IR}$ with large values and opposite signs. This would mean that the two corresponding contributions to the canonical part of BSR, $d(Q^2)$, are large and have opposite signs, giving possible strong cancellations, which would be an unexpected behaviour.

The expectation, based on the arguments in Refs. [40, 41], is that the leading IR renormalon contribution (IR$_1$: $\propto \widetilde{d}_1^{\rm IR}$) gives us the dominant contribution to $d(Q^2)$, and that the subleading IR contribution (IR$_2$: $\propto \widetilde{d}_2^{\rm IR}$) as well as the UV renomalon contributions (UV$_j$: $\propto \widetilde{d}_j^{\rm UV}$; $j = 1, 2$) all give numerically subdominant contributions to $d(Q^2)$. This is evidently not the case in our obtained renormalon-model resummation (3.55) in the $\overline{\rm MS}$ scheme as seen in Table 3.1. Therefore, we will vary the renormalisation scheme (via the leading renormalisation-scheme parameters $c_k \equiv \beta_k/\beta_0$; $k = 2, 3$) in such a way as to achieve the expected hierarchy of the four different renormalon contributions.

As mentioned earlier, the quantity $d(Q^2)$ must be renormalisation scale and scheme independent, so one may think that the resummed results (3.55) must be too. The evaluated resummed quantity is exactly renormalisation scale independent, as mentioned above. However, it is not scheme independent (i.e., β_j-independent, where $j \geq 2$). This is so because the expression (3.3) for $\mathcal{B}[\widetilde{d}](u)$ in general does not contain all the terms. As was alluded to at the start of Chapter 3, the anomalous dimensions corresponding to the three renormalons where $u = 2, -1, -2$ were taken to be zero (as are in the large-β_0 limit) and consequently the corresponding singularity structures there were taken to be simple poles. In reality, these terms are expected to be different from simple poles. Further, for each such term $1/(p \mp u)^\kappa$ in $\mathcal{B}[\widetilde{d}](u)$ we expect to have other, subleading terms $\sim 1/(p \mp u)^{\kappa-1}$, and those terms were not included either, i.e., they were "truncated out" because of lack of information. The five-parameter *ansatz* (3.3) is therefore a simplified and truncated version, in which we were able to determine the parameters on the basis of the information about the pQCD perturbation series (2.10) truncated at $\sim \widetilde{a}_5 \sim a^5$. Hence, we cannot expect that our

resummed results (3.55) are invariant under scheme variation and, additionally, we will have uncertainties of the extracted parameter values from scheme variation.

The procedure is as follows. We vary the scheme, by varying the c_2 and c_3 scheme parameters (where $c_j \equiv \beta_j/\beta_0$). There are also other, more subleading, scheme parameters β_j (or $c_j \equiv \beta_j/\beta_0$) ($j \geq 3$). For convenience, we vary only the first two c_j ($j = 2, 3$) and construct the beta-function with such c_j which allows an explicit solution for the running coupling $a(Q^2; c_2, c_3)$ in terms of the Lambert function as seen in Ref. [42]. The corresponding beta-function $\beta(a)$ has a Padé $[4/4](a)$ ('P44') form, i.e., $\beta(a)$ is a coefficient of two polynomials of a, each of them of degree 4

$$\frac{da(Q^2)}{d\ln Q^2} = \beta(a(Q^2)) \equiv -\beta_0 a(Q^2)^2 \frac{[1 + a_0 c_1 a(Q^2) + a_1 c_1^2 a(Q^2)^2]}{[1 - a_1 c_1^2 a(Q^2)^2]\,[1 + (a_0 - 1) c_1 a(Q^2) + a_1 c_1^2 a(Q^2)^2]}\,, \tag{4.1}$$

where $c_j \equiv \beta_j/\beta_0$ and

$$a_0 = 1 + \sqrt{c_3/c_1^3}, \quad a_1 = c_2/c_1^2 + \sqrt{c_3/c_1^3}. \tag{4.2}$$

Expansion of this β-function up to $\sim a(Q^2)^5$ gives the expression (2.5) in terms of only c_2 and c_3. In Ref. [42] it was shown that the RGE (4.1) has explicit solutions in terms of the Lambert functions $W_{\mp 1}(z)$

$$a(Q^2) = \frac{2}{c_1}\left[-\sqrt{\omega_2} - 1 - W_{\mp 1}(z) + \sqrt{(\sqrt{\omega_2} + 1 + W_{\mp 1}(z))^2 - 4(\omega_1 + \sqrt{\omega_2})}\right]^{-1}, \tag{4.3}$$

where $\omega_1 = c_2/c_1^2$, $\omega_2 = c_3/c_1^3$, $Q^2 = |Q^2|\exp(i\phi)$. The Lambert function W_{-1} is used when $0 \leq \phi < \pi$, and W_{+1} when $-\pi \leq \phi < 0$. Also, we have

$$z \equiv z(Q^2) = -\frac{1}{c_1 e}\left(\frac{\Lambda_L^2}{Q^2}\right)^{\beta_0/c_1}. \tag{4.4}$$

Where scale Λ_L is the so called Lambert scale ($\Lambda_L \sim \Lambda_{\rm QCD}$). The class of schemes that have the explained formulation are called 'P44' schemes. The coupling (4.3), is also the used in the resummation (3.55), and has $n_f = 3$, because this resummation corresponds to the perturbation expansion (2.10) or equivalently (2.1) of BSR at low Q^2 where $n_f = 3$. The coupling (4.3) is determined by the value of $\alpha_s(M_Z^2; \overline{\rm MS})$ (which is defined at $N_f = 5$) via the 5-loop $\overline{\rm MS}$ RGE running and the corresponding quark threshold relations, and by thus changing the scheme from (5-loop) $\overline{\rm MS}$ to the

'P44' scheme at $Q^2 = (2\bar{m}_c)^2 - 0$ (with $N_f = 3$) by some known transformations (see Appendix D of [10]).

For example, when we choose the P44 scheme with the $\overline{\rm MS}$ values of c_2 and c_3, the parameters of $\mathcal{B}[\widetilde{d}](u)$ are those in the second row of Table 4.1, and we get results very close to the 5-loop $\overline{\rm MS}$ case (first row therein). The resummed $d(Q^2)$ expression (3.55), at $Q^2 = 3$ GeV^2, divided in its separate renormalon contributions is given in the last row of Table 4.2 in this (P44) $\overline{\rm MS}$ case, which shows that the two IR contributions are large and with strong cancellation. For this reason, we will consider such a scheme as unacceptable in our approach.

We, for the reasons explained earlier in this section, need a certain hierarchy of the renormalon contributions so that our resummed result adjusts to the theoretically expected behaviour. Thus, we will confine ourselves to the schemes (P44-class) which give us the following type of contributions to $d(Q^2)$:

1. The IR ($u = 1$) renormalon contribution $d(Q^2)_{\rm IR1}$ is the dominant contribution.
2. The rescaling parameter $\widetilde{K}$ in $\mathcal{B}[\widetilde{d}](u)$ is $|\widetilde{K}| < 1$.
3. The IR ($u = 2$) renormalon contribution $d(Q^2)_{\rm IR2}$ is in the range $0 < d(Q^2)_{\rm IR2} < d(Q^2)_{\rm IR1}$
4. The UV ($u = -2$) renormalon contribution $d(Q^2)_{\rm UV2}$ should not be too large: $|\widetilde{d}_2^{\rm UV}| < 0.5$.

The conditions 2. and 3. turn out to be related: when $d(Q^2)_{\rm IR2} < 0$, we usually have $|\widetilde{K}| > 1$, and $d(Q^2)_{\rm IR1}$ and $d(Q^2)_{\rm IR2}$ are large and with opposite signs and thus largely cancel. Taking into account these conditions, we obtain as acceptable (P44)-schemes those with

$$c_2 = 9^{+2}_{-1.4}, \quad c_3 = 20 \pm 15. \tag{4.5}$$

We note that when c_2 goes below the value $(9-1.4)$, the value of $|\widetilde{K}|$ becomes suddenly large and we once again obtain strong cancellations of $d(Q^2)_{\rm IR1}$ and $d(Q^2)_{\rm IR2}$.

In Tables 4.2 and 4.3 we present the results for these P44 schemes, when c_2 and c_3 have the central values, or one of them varies to an edge value given in Eqs. (4.5): In the first case the parameters of $\mathcal{B}[\widetilde{d}](u)$, and in the second the decomposition of $d(Q^2)$ into the four renormalon contributions.

Table 4.2: The values of parameters of the five-parameter *ansatz* (3.3) in the P44 renormalisation schemes, for various scheme parameters c_2 and c_3. Included are also the corresponding numerical values of the canonical BSR $d(Q^2)$ for the renormalon-motivated resummation (3.55), at $Q^2 = 3$ GeV^2 (and $N_f = 3$) and for $\alpha_s(M_Z^2; \overline{\rm MS}) = 0.1179$. The coefficient d_4 corresponds to the 5-loop $\overline{\rm MS}$ coefficient value $d_4(\overline{\rm MS}) = 1557.43$ as predicted by ECH.

c_2	c_3	$\widetilde{K}$	$\widetilde{d}_1^{\rm IR}$	$\widetilde{d}_2^{\rm IR}$	$\widetilde{d}_1^{\rm UV}$	$\widetilde{d}_2^{\rm UV}$	$d(Q^2)$
9.	20.	0.450041	0.331813	0.231437	-0.0809782	0.0964868	0.1816
7.6	20.	0.896252	0.210843	0.137235	-0.158441	0.394581	0.1843
11.0	20.	0.12894	0.422324	0.301175	-0.015641	-0.477922	0.1807
9.	5.	0.359327	0.474866	-0.026115	-0.080151	-0.126694	0.1737
9.	35.	0.484948	0.237256	0.431189	-0.067963	-0.133156	0.1888
$c_2^{\overline{\rm MS}}$	$c_3^{\overline{\rm MS}}$	-1.83223	7.86652	-14.9299	-0.0444416	-0.0776748	0.1632

Table 4.3: The values of the corresponding numerical values of the canonical BSR $d(Q^2)$ as well as its numerical decomposition to the four renormalon contributions, for the renormalon-motivated resummation (3.55), at $Q^2 = 3$ GeV^2 (and $N_f = 3$) and for $\alpha_s(M_Z^2; \overline{\rm MS}) = 0.1179$, for various scheme parameters c_2 and c_3 in the P44 renormalisation schemes covering the intervals Eq. (3.3). The coefficient d_4 corresponds to the 5-loop $\overline{\rm MS}$ coefficient value $d_4(\overline{\rm MS}) = 1557.43$ as predicted by ECH.

c_2	c_3	$d(Q^2)$	$d(Q^2)_{\rm IR1}$	$d(Q^2)_{\rm IR2}$	$d(Q^2)_{\rm UV1}$	$d(Q^2)_{\rm UV2}$
9.	20.	0.1816	0.1631	0.0597	-0.0247	-0.0164
7.6	20.	0.1843	0.1196	0.0421	-0.0551	0.0777
11.0	20.	0.1807	0.1904	0.0701	-0.0044	-0.0752
9.	5.	0.1737	0.2243	-0.0064	-0.0236	-0.0207
9.	35.	0.1888	0.1188	0.1143	-0.0212	-0.0232
$c_2^{\overline{\rm MS}}$	$c_3^{\overline{\rm MS}}$	0.1632	1.9466	-1.7675	-0.0082	-0.0076

In Fig. 4.1 we present the resummed results for the canonical BSR part $d(Q^2)$ of the OPE Eq. (3.1), Eq. (3.55), for the considered central case of renormalisation scheme (P44 with $c_2 = 9.$ and $c_3 = 20.$) and with the strength of the coupling corresponding to the known value $\alpha_s(M_Z^2; \overline{\text{MS}}) = 0.1179$ (giving $\Lambda_L = 0.2175$ GeV), as seen in [9] and further expanded in [10].

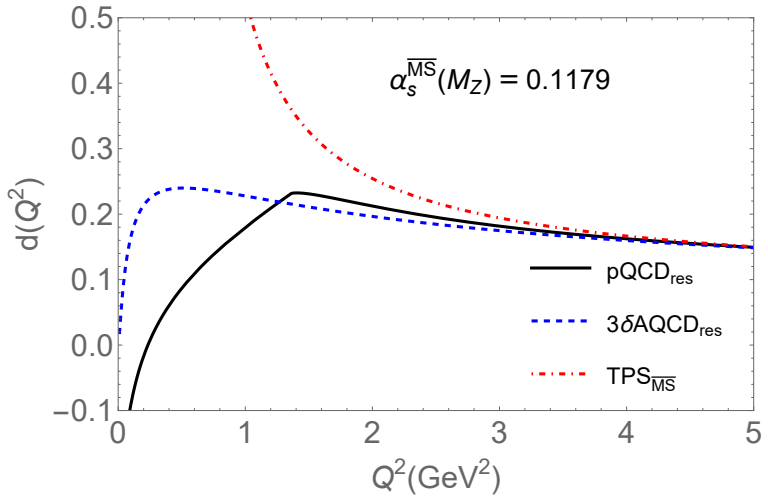

Figure 4.1: The resummed canonical part of the BSR, $d(Q^2)_{\text{res}}$, according to Eq. (3.55), in the 'P44' renormalisation scheme with $c_2 = 9.$ and $c_3 = 20.$, for $N_f = 3$ ('pQCD$_{\text{res}}$'). The strength of the coupling is determined by $\alpha_s(M_Z^2; \overline{\text{MS}}) = 0.1179$. The resummation with the corresponding 3δAQCD coupling is included, for comparison ('3dAQCD$_{\text{res}}$'). Further, we include the evaluation as the truncated perturbation series (TPS) in powers of $a = a(Q^2)$ in $\overline{\text{MS}}$ scheme, up to $\sim a^5$ term and with the corresponding coefficient, $d_4^{\overline{\text{MS}}} = 1557.4$ ('TPS$_{\overline{\text{MS}}}$'). Graphic as obtained in [9], more comparisons can be found in [10].

We can clearly see in this Figure that the pQCD curve loses its expected behaviour for $Q^2 < 1.44$ GeV^2 with a soft kink. This occurs because for such low Q^2 the effects of the Landau singularities of the pQCD running coupling $a(te^{-\widetilde{K}}Q^2 + i\epsilon)$ in the integral (3.55) become significant. We conclude that the used renormalon-motivated resummation in the considered scheme starts failing at $Q^2 < 1.44$ GeV^2 due to the Landau singularities of the pQCD running coupling. This motivates the use in our works (though not detailed in this thesis) of some AQCD variants to get better performance out of our chosen method of resummation.

In Fig. 4.1 we included, for comparison, the results of the resummation Eq. (3.56) when the coupling $a(Q^2) \mapsto \mathcal{A}(Q^2)$ is holomorphic (i.e. without Landau singularities). We used a specific 3δAQCD coupling, for the case $\alpha_s(M_Z^2; \overline{\text{MS}}) = 0.1179$ and with the spectral function $\rho(\sigma) \equiv \text{Im}\mathcal{A}(-\sigma - i\epsilon)$, for details see [31, 32]. We see that in

the 3δAQCD case the resummation converges quite rapidly to the pQCD values with higher Q^2 but, although it does not have a kink as the pQCD, it does tend to zero quite rapidly at very low Q^2. Also for comparison we included in the figure the pQCD truncated perturbation series (TPS) curve in the $\overline{\text{MS}}$ scheme (with $\kappa = 1$), which has the bizarre behaviour of becoming infinite at around $Q^2 \approx 0.40$ GeV^2, which is the branching point of the unphysical Landau cut of the pQCD coupling. The TPS curve does not exist for $Q^2 < 0.40$ GeV^2. This clearly shows that the use of the pQCD resummed approach from our work already considerably improves the results for low energies when compared to the usual approach of simply truncated series.

4.2 Fitting to Experimental Data

In Figs. 4.2 we present the numerical results for the inelastic BSR $\overline{\Gamma}_1^{p-n}(Q^2)$ from various experiments [17–23], with the statistical and systematic uncertainties.

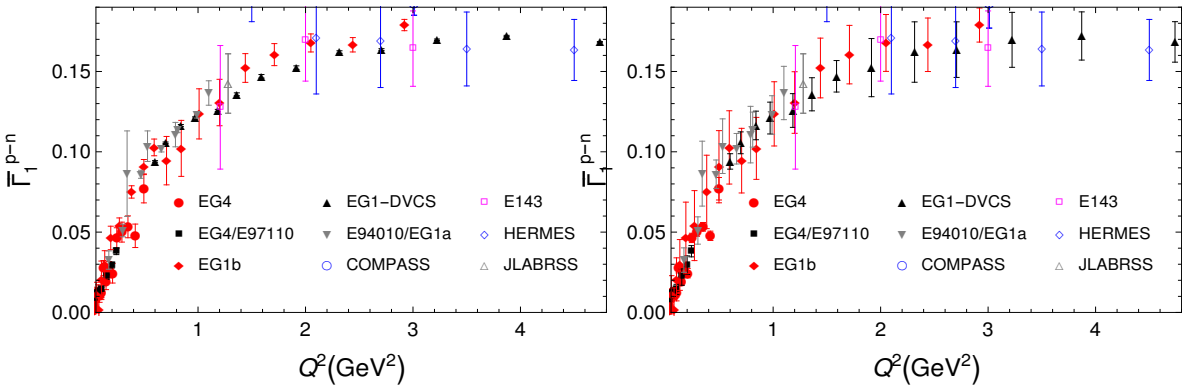

Figure 4.2: The measured results for the inelastic BSR $\overline{\Gamma}_1^{p-n}(Q^2)$ for different experiments [17–23], with the statistical (left Figure) and systematic (right Figure) uncertainties, as presented in Refs. [9, 10].

We will perform the fit by using for $d(Q^2)$ the resummed expression (3.55) with the ($n_f = 3$) pQCD coupling in the P44-type renormalisation scheme where $c_2 = 9.$ and $c_3 = 20.$, such that it corresponds to $\alpha_s(M_Z^2; \overline{\text{MS}}) = 0.1179$ ($n_f = 5$) which is the central value of the world average [39]. The fit parameters will be either $\bar{f}_2$ or ($\bar{f}_2$, μ_6), i.e. we truncate the OPE (1.8) at $D = 2$ or $D = 4$ respectively.

We do not know which experimental uncertainties are correlated and which are not. The statistical uncertainties could be uncorrelated, but the correlations of the

systematic uncertainties are expected to be considerable and difficult to estimate. Therefore, we follow the method of unbiased estimate [11, 43, 44] which tries to minimise a certain parameter k (also see for details the corresponding fit section in [10]). In practice, we always obtain $0 < k < 0.5$. The experimental uncorrelated uncertainty (exp.u.) of the extracted parameters is then obtained by the conventional methods (See for example Appendix of Ref. [45]). The correlated experimental uncertainties (exp.c.) are then obtained by shifting the central experimental values $\overline{\Gamma}_1^{p-n}(Q_j^2)$ by $(1-\sqrt{k})\sigma_{\rm sys}(Q_j^2)$ up and down and redoing the fit for these values.

We point out that the smaller the obtained value of k, the better the fit. It turns out that, in the above approach, the results depend considerably on the value of $Q^2_{\rm min}$ that we choose. We chose $Q^2_{\rm min} = 1.71$ GeV^2 for the fit with two parameters ($\bar{f}_2$, μ_6) for the following reasons:

1. If we decrease $Q^2_{\rm min}$ to the adjacent lower neighbouring data points, the value of k increases.

2. If we decrease $Q^2_{\rm min}$ one step further, to 1.44 GeV^2, then we can see numerically that the evaluation of $d(Q^2)$ via Eq. (3.55) is already on the border of applicability at such Q^2, due to the effects of the Landau singularities of the coupling $a(te^{-\widetilde{K}}Q^2 + i\epsilon)$ in the integral, as seen in Fig. 4.1.

3. If we increase $Q^2_{\rm min}$ above 1.71 GeV^2 to the upper neighbour 1.915 GeV^2, the value of k increases (to $k = 0.180$).

4. If we increase $Q^2_{\rm min}$ even further, we obtain the results with strong cancellations between the $D = 2$ and $D = 4$ terms.

For all these reasons, we choose $Q^2_{\rm min} = 1.71^{+0.205}_{-0.27}$ GeV^2, and the value of k parameter is $k = 0.1621$.

If the fit is performed only with one fit parameter ($\bar{f}_2$), similar estimations give us $Q^2_{\rm min} = 1.71^{+0.39}_{-0.27}$ GeV^2, and the value of k parameter is $k = 0.1487$.

With the approach described above, we obtain the final result for the fits. For the

two-parameter fit the result is $k = 0.1621$ and

$$\begin{aligned} \bar{f}_2 &= -0.160^{-0.007}_{+0.025}(c_2)^{+0.054}_{-0.039}(c_3)^{+0.044}_{-0.041}(\alpha_s)^{-0.012}_{+0.016}(d_4) \mp 0.043(\text{ren}) \\ &\quad {}^{+0.016}_{+0.119}(Q^2_{\text{min}}) \pm 0.160(\text{exp.u.}) \pm 0.297(\text{exp.c.}), \qquad (4.6a) \\ \mu_6 &= +0.022^{+0.003}_{-0.008}(c_2)^{-0.013}_{+0.004}(c_3)^{-0.010}_{+0.008}(\alpha_s)^{+0.002}_{-0.003}(d_4) \mp 0.010(\text{ren}) \\ &\quad {}^{-0.006}_{-0.053}(Q^2_{\text{min}}) \pm 0.062(\text{exp.u.}) \mp 0.059(\text{exp.c.}) \ [\text{GeV}^4]. \qquad (4.6b) \end{aligned}$$

The quantity μ_6 is in units of GeV^4. Here, the uncertainties at '(c_2)' and '(c_3)' come from renormalisation scheme variation Eq. (4.5). The uncertainty at '(α_s)' comes from the world average uncertainty $\alpha_s(M_Z^2; \overline{\text{MS}}) = 0.1179 \pm 0.0009$ [39]. The uncertainty at '(d_4)' comes from the variation of d_4 in such a way that the corresponding (5-loop) $\overline{\text{MS}}$ value $d_4^{\overline{\text{MS}}}$ varies according to its known range. The uncertainty at '(ren)' is the renormalon uncertainty, it appears when in the evaluation of $d(Q^2)$, Eq. (3.55), we add or subtract the same integral, but only imaginary part (divided by π) instead of the real part $[\pm(1/\pi)\text{Im}(\ldots)]$. These are all the theoretical uncertainties.

The uncertainty at '(Q^2_{min})' can be regarded as coming primarily from experimental uncertainties, and it originates from the variation $Q^2_{\text{min}} = 1.71^{+0.205}_{-0.27}$ GeV^2 as mentioned above. The experimental uncertainties at '(exp.u.)' and '(exp.c.)' were addressed in the previous paragraphs.

The one-parameter fit ($\bar{f}_2$) gives, on the other hand, $k = 0.1487$ and

$$\begin{aligned} \bar{f}_2 &= -0.107^{-0.001}_{+0.007}(c_2)^{+0.022}_{-0.029}(c_3) \pm 0.020(\alpha_s) \mp 0.009(d_4) \mp 0.067(\text{ren}) \\ &\quad {}^{+0.012}_{-0.029}(Q^2_{\text{min}}) \pm 0.033(\text{exp.u.}) \pm 0.154(\text{exp.c.}), \qquad (4.7) \end{aligned}$$

Here, the uncertainty (Q^2_{min}) comes from $Q^2_{\text{min}} = 1.71^{+0.39}_{-0.27}$ GeV^2 as mentioned above.

If we did not include the charm decoupling violation term $\delta d(Q^2)_{m_c}$, Eq. (3.2), in our analysis, then the results would change very little and all the uncertainties would remain practically unchanged (see [9]). The k parameter values would change from 0.1621 and 0.1487 to 0.1626 and 0.1493, respectively, which means the fit would be only very slightly worse.

The above results show that we have a competition between various theoretical uncertainties (which are in general moderate), and various experimental uncertainties of the extracted values which are large and are in general dominant over the theoretical uncertainties. The experimental uncertainties of the extracted parameter values have

their origin, directly or indirectly, in the large statistical and systematic uncertainties of the BSR data points. The large experimental uncertainties of the data points make the deduction of the preferred value of α_s from the BSR data practically impossible, and hence we took the world average data for α_s [39].

In Figure 4.3 we present the obtained fits $\bar{\Gamma}_1^{p-n}(Q^2; \bar{f}_2, \mu_6)$ and $\bar{\Gamma}_1^{p-n}(Q^2; \bar{f}_2)$ in pQCD using the OPE terms from Eq. 3.1 with the central fit values of Eqs. (4.6, 4.7). For comparison, the experimental data points are included.

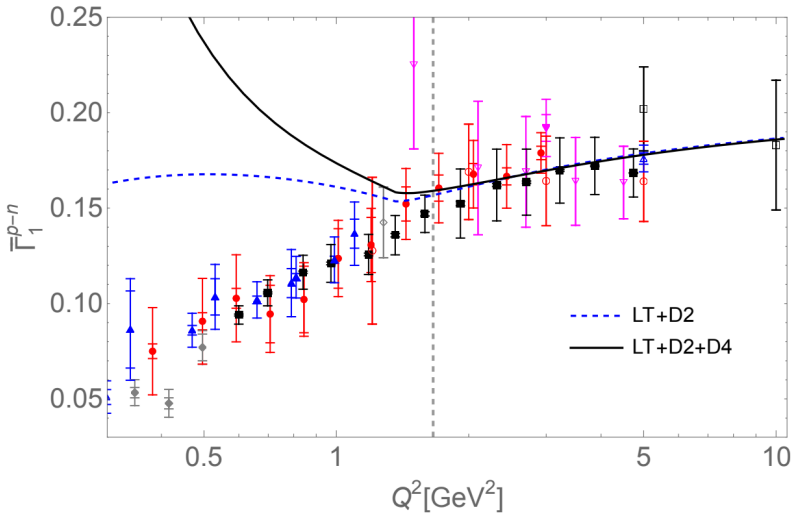

Figure 4.3: Fitted curves $\bar{\Gamma}_1^{p-n}(Q^2; \bar{f}_2, \mu_6)$ and $\bar{\Gamma}_1^{p-n}(Q^2; \bar{f}_2)$, for the one-parameter (LT+D2) and two-parameter (LT+D2+D4). The coupling used is that of pQCD. Experimental data points are included for comparison. The vertical line indicates the value of the left end of the fit, $Q^2_{\text{min}} = 1.71$ GeV^2. Figure from [10].

It is clear from the figure that although the behaviour of the obtained quantity when including the further OPE terms to our resummation is better than that of using only the canonical part (from Fig. 4.1), but it is still far from the experimental data for $Q^2 < Q^2_{\text{min}}$. This is because we are still using the pQCD coupling that has Landau singularities in the very low Q^2 regime.

4.3 Using the Method with AQCD

Due to the problems with the coupling seen in the two previous sections, there is room for improvement in the results of our resummation approach by the use of holomorphic variants of the QCD coupling such as those mentioned in Section 1.5, which don't have Landau singularities, that make the evaluation of the integral of the resummation Eq. (3.55) not have ambiguities and thus enhance our predictions. This was done and presented in Ref. [9] for 3δAQCD (developed in [31, 32]) only for comparison with the pQCD resummation, and for both 2δAQCD (developed in [30]) and 3δAQCD in Ref. [10] with a much deeper analysis. We present here those results, analogous to those resummed with pQCD, though for comparison purposes only, as this is not the focus of this thesis (for details in how these AQCD variants were constructed see Appendix F of [10]). We note that the process is very similar from the previous case so we do not reproduce them here.

In Figures 4.4 we present the resulting fitted curves for $\bar{\Gamma}_1^{p-n}(Q^2; \bar{f}_2, \mu_6)$ and $\bar{\Gamma}_1^{p-n}(Q^2; \bar{f}_2)$ with our resummation method in 2δAQCD and 3δAQCD.

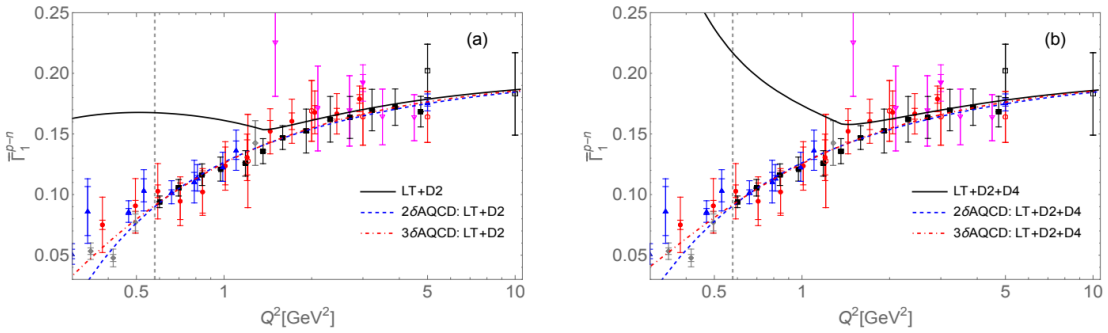

Figure 4.4: Fitted curves for the BSR $\bar{\Gamma}_1^{p-n}(Q^2)$: (a) for the one-parameter fit; (b) for the two-parameter fit. The couplings used are those of 2δAQCD and 3δAQCD. Experimental data points, and the pQCD fit from Fig. 4.3 are included for comparison. The vertical line is the limit of the left end of the fit for the AQCD curves, $Q^2_{\text{min}} = 0.592$ GeV^2. Figure from [10]

We can see from the figures that using the resummation method explored in this work with any of the two mentioned AQCD variants significantly enhances the coincidence of the obtained results to the experimental data, at least visually, especially in the region $Q^2 \lesssim Q^2_{\text{min}}$. This is especially notorious when comparing with the resummation using the pQCD coupling from Fig. 4.3.

Chapter 5

Conclusions and Future

In this work, we explored the reasons that motivate the use of methods different from the usual perturbation theory approach when we want to evaluate QCD observables in the low-energy, long-distance, infrared regime. In particular, we studied, outlined, and applied to the polarised Bjorken Sum Rule a specific method [8] that prescribes the evaluation of the canonical QCD part of observables through a resummation based on the known renormalon structure of those observables, as well as the use of the OPE form of them to enhance the mentioned resummation and perform fits to data (when available, as is the case for the BSR). The resummation can be performed (and has been) both with the usual pQCD coupling and with those of AQCD variants like 2δAQCD and 3δAQCD. This resummation was also proved to be invariant under renormalisation scale variation (though this is not the case under scheme variation).

The method chosen can be summarised as follows: First, we constructed the expansion series and its logarithmic derivative analogue for our observable $d(Q^2)$ (in this case the BSR); then, the Borel transform of these quantities were generated which, coupled to the renormalon structure of the observable, allowed us to make an *ansatz* for the modified Borel transform with which to fix its parameters by using the known perturbative coefficients; afterwards, we computed the full characteristic function that turns out is the inverse Mellin transform of the previously mentioned transform, and then used it to perform the renormalon-based extension of the canonical part of the observable, which was our goal; finally, we explored how renormalisation scheme variation alters our resummation results, and how our results can be extended in OPE and used to fit to experimental data.

In particular and in a very detailed way, we studied the specifics of performing the resummation of the canonical $d(Q^2)$ part of the polarised Bjorken Sum Rule, as seen in Chapter 3, especially the contour integrals necessary to evaluate the resummation characteristic function due to the renormalon structure. These details were not contained in previous publications, they were only alluded to in general, and thus are novel. This full application of that part of the Cvetič method shows that the use of the modified Borel transform $\mathcal{B}[\tilde{d}](u)$ and the modified coefficients $\tilde{d}_n(\kappa)$ brings about a simpler structure for the associated integrals which makes the use of the renormalon structure more straightforward than the original version of those. This in turn allows for the resummation itself to be performed in a simple way, and the results show that using resummation makes the evaluation much better than just truncating the perturbation series, especially when using AQCD couplings that have no Landau singularities.

With the results shown in this work, from [9, 10], it was well established that using a renormalon-based resummation is more reliable than plain truncation of the expansion and that this method fulfils our desired conditions from Section 1.6, and even more so when using AQCD couplings. The results and experience therefore leads us to conclude that for observables like the BSR for which we know the renormalon structure, the method studied improves the theoretical description of the observables through its use of resummation , and highlights the possibility of using holomorphic couplings that have no singularities but are compatible with the original pQCD couplings at higher energies.

It only remains, then, to keep testing this promising method at low energies with other spacelike QCD observables whose renormalon structure is known and for which there are experimental data available to compare.

References

[1] M. Gell-Mann. A schematic model of baryons and mesons. *Physics Letters*, 8:214–215, 2 1964.

[2] G Zweig. An SU_3 model for strong interaction symmetry and its breaking; Version 2. 1964. CERN Preprint, DOI: 10.17181/CERN-TH-412.

[3] H. Fritzsch, M. Gell-Mann, and H. Leutwyler. Advantages of the color octet gluon picture. *Physics Letters B*, 47:365–368, 11 1973.

[4] David J. Gross and Frank Wilczek. Ultraviolet Behavior of Non-Abelian Gauge Theories. *Physical Review Letters*, 30:1343–1346, 6 1973.

[5] H. David Politzer. Reliable Perturbative Results for Strong Interactions? *Physical Review Letters*, 30:1346–1349, 6 1973.

[6] J. D. Bjorken. Applications of the Chiral U(6) x (6) Algebra of Current Densities. *Phys. Rev.*, 148:1467–1478, 1966.

[7] J. D. Bjorken. Inelastic Scattering of Polarized Leptons from Polarized Nucleons. *Physical Review D*, 1:1376–1379, 3 1970.

[8] Gorazd Cvetič. Renormalon-motivated evaluation of QCD observables. *Physical Review D*, 99:014028, 1 2019.

[9] Cesar Ayala, Camilo Castro-Arriaza, and Gorazd Cvetič. Evaluation of Bjorken polarised sum rule with a renormalon-motivated approach. *Phys. Lett. B*, 848:138386, 2024.

[10] César Ayala, Camilo Castro-Arriaza, and Gorazd Cvetič. Renormalon-based resummation of Bjorken polarised sum rule in perturbative and holomorphic QCD. 12 2023. https://doi.org/10.48550/arXiv.2312.13134.

[11] P.A. Zyla et al. Review of Particle Physics. *Progress of Theoretical and Experimental Physics*, 2020, 8 2020.

[12] Alexandre Deur, Stanley J. Brodsky, and Guy F. de Teramond. The QCD Running Coupling. *Nucl. Phys.*, 90:1, 2016.

[13] David J. Gross and André Neveu. Dynamical symmetry breaking in asymptotically free field theories. *Phys. Rev. D*, 10:3235–3253, Nov 1974.

[14] B. E. Lautrup. On High Order Estimates in QED. *Phys. Lett. B*, 69:109–111, 1977.

[15] G. 't Hooft. Can we make sense out of "quantum chromodynamics"? *The Whys of Subnuclear Physics*, page 943–982, 1979.

[16] M. Beneke. Renormalons. *Phys. Rept.*, 317:1–142, 1999.

[17] B. Adeva et al. The spin-dependent structure function $g_1(x)$ of the proton from polarized deep-inelastic muon scattering. *Physics Letters B*, 412:414–424, 10 1997.
D. Adams et al. Spin structure of the proton from polarized inclusive deep-inelastic muon-proton scattering. *Physical Review D*, 56:5330–5358, 11 1997.
E.S. Ageev et al. Measurement of the spin structure of the deuteron in the DIS region. *Physics Letters B*, 612:154–164, 4 2005.
V. Yu. Alexakhin et al. The Deuteron Spin-dependent Structure Function g_1^d and its First Moment. *Phys. Lett. B*, 647:8–17, 2007.
M. G. Alekseev et al. The Spin-dependent Structure Function of the Proton g_1^p and a Test of the Bjorken Sum Rule. *Phys. Lett. B*, 690:466–472, 2010.
C. Adolph et al. The spin structure function g_1^{p} of the proton and a test of the Bjorken sum rule. *Phys. Lett. B*, 753:18–28, 2016.
C. Adolph et al. Final COMPASS results on the deuteron spin-dependent structure function g_1^{d} and the Bjorken sum rule. *Phys. Lett. B*, 769:34–41, 2017.
M. Aghasyan et al. Longitudinal double-spin asymmetry A_1^{p} and spin-dependent structure function g_1^{p} of the proton at small values of x and Q^2. *Phys. Lett. B*, 781:464–472, 2018.

[18] K. Ackerstaff et al. Measurement of the neutron spin structure function g with a polarized ^{3}He internal target. *Physics Letters B*, 404:383–389, 7 1997.

A. Airapetian et al. Measurement of the proton spin structure function g_1^p with a pure hydrogen target. *Physics Letters B*, 442:484–492, 12 1998.

[19] P. L. Anthony et al. Deep inelastic scattering of polarized electrons by polarized ^{3}He and the study of the neutron spin structure. *Physical Review D*, 54:6620–6650, 12 1996.
K. Abe et al. Precision Determination of the Neutron Spin Structure Function g_1^n. *Physical Review Letters*, 79:26–30, 7 1997.
K. Abe et al. Measurements of the proton and deuteron spin structure functions g_1 and g_2. *Physical Review D*, 58:112003, 10 1998.
P.L. Anthony et al. Measurement of the deuteron spin structure function $g_1^d(x)$ for 1 $(\mathrm{GeV/c})^2 < Q^2 < 40$ $(\mathrm{GeV/c})^2$. *Physics Letters B*, 463:339–345, 9 1999.
P.L Anthony et al. Measurements of the Q^2-dependence of the proton and neutron spin structure functions g_1^p and g_1^n. *Physics Letters B*, 493:19–28, 11 2000.

[20] A. Deur et al. Experimental Determination of the Evolution of the Bjorken Integral at Low Q^2. *Physical Review Letters*, 93:212001, 11 2004.
A. Deur et al. Experimental study of isovector spin sum rules. *Physical Review D*, 78:032001, 8 2008.

[21] K. Slifer et al. Probing Quark-Gluon Interactions with Transverse Polarized Scattering. *Physical Review Letters*, 105:101601, 9 2010.

[22] A. Deur et al. High precision determination of the Q^2 evolution of the Bjorken sum. *Physical Review D*, 90:012009, 7 2014.

[23] K. P. Adhikari et al. Measurement of the Q^2 Dependence of the Deuteron Spin Structure Function g_1 and its Moments at Low Q^2 with CLAS. *Phys. Rev. Lett.*, 120(6):062501, 2018.
X. Zheng et al. Measurement of the proton spin structure at long distances. *Nature Physics*, 17:736–741, 6 2021.

[24] S.G. Gorishny and S.A. Larin. Qcd corrections to the parton-model sum rules for structure functions of deep inelastic scattering. *Physics Letters B*, 172:109–112, 5 1986.

[25] S. A. Larin and J. A. M. Vermaseren. The α_s^3 corrections to the Bjorken sum rule for polarized electroproduction and to the Gross-Llewellyn Smith sum rule. *Phys. Lett. B*, 259:345–352, 1991.

[26] P. A. Baikov, K. G. Chetyrkin, and J. H. Kuhn. Adler Function, Bjorken Sum Rule, and the Crewther Relation to Order α_s^4 in a General Gauge Theory. *Phys. Rev. Lett.*, 104:132004, 2010.

[27] Stanley J. Brodsky, Guy F. de Teramond, and Alexandre Deur. Nonperturbative QCD Coupling and its β-function from Light-Front Holography. *Phys. Rev. D*, 81:096010, 2010.

[28] Alexandre Deur, Jian-Ming Shen, Xing-Gang Wu, Stanley J. Brodsky, and Guy F. de Téramond. Implications of the principle of maximum conformality for the QCD strong coupling. *Physics Letters B*, 773:98–104, 10 2017.

[29] D. V. Shirkov and I. L. Solovtsov. Analytic QCD running coupling with finite IR behaviour and universal $\{\bar{\alpha}\}_s(0)$ value. 4 1996.

[30] César Ayala, Carlos Contreras, and Gorazd Cvetič. Extended analytic QCD model with perturbative QCD behavior at high momenta. *Physical Review D*, 85:114043, 6 2012.

[31] César Ayala, Gorazd Cvetič, Reinhart Kögerler, and Igor Kondrashuk. Nearly perturbative lattice-motivated QCD coupling with zero IR limit. *Journal of Physics G: Nuclear and Particle Physics*, 45:035001, 3 2018.

[32] Gorazd Cvetič and Reinhart Kögerler. Lattice-motivated QCD coupling and hadronic contribution to muon $g-2$. *Journal of Physics G: Nuclear and Particle Physics*, 48(5):055008, 2021.

[33] Gorazd Cvetic and Cristian Valenzuela. Analytic QCD: A Short review. *Braz. J. Phys.*, 38:371–380, 2008.

[34] D.J. Broadhurst and A.L. Kataev. Connections between deep-inelastic and annihilation processes at next-to-next-to-leading order and beyond. *Physics Letters B*, 315:179–187, 9 1993.

[35] César Ayala, Gorazd Cvetič, and Diego Teca. Borel–Laplace sum rules with τ decay data, using OPE with improved anomalous dimensions. *Journal of Physics G: Nuclear and Particle Physics*, 50:045004, 4 2023.

[36] Matthias Neubert. Scale setting in QCD and the momentum flow in Feynman diagrams. *Physical Review D*, 51:5924–5941, 5 1995.

[37] Matthias Neubert. Resummation of renormalon chains for cross-sections and inclusive decay rates. 2 1995.

[38] Johannes Blümlein, Giulio Falcioni, and Abilio De Freitas. The Complete $O(\alpha_s^2)$ Non-Singlet Heavy Flavor Corrections to the Structure Functions $g_{1,2}^{ep}(x,Q^2)$, $F_{1,2,L}^{ep}(x,Q^2)$, $F_{1,2,3}^{\nu(\bar{\nu})}(x,Q^2)$ and the Associated Sum Rules. *Nucl. Phys. B*, 910:568–617, 2016.

[39] R L Workman et al. Review of particle physics. *Progress of Theoretical and Experimental Physics*, 2022, 8 2022.

[40] Francisco Campanario and Antonio Pineda. Fit to the bjorken, ellis-jaffe and gross-llewellyn-smith sum rules in a renormalon based approach. *Physical Review D*, 72:056008, 9 2005.

[41] Cesar Ayala and Antonio Pineda. Bjorken sum rule with hyperasymptotic precision. *Physical Review D*, 106:056023, 9 2022.

[42] Gorazd Cvetič and Igor Kondrashuk. Explicit solutions for effective four- and five-loop qcd running coupling. *Journal of High Energy Physics*, 2011:19, 12 2011.

[43] A. Deur, J.P. Chen, et al. Experimental study of the behavior of the bjorken sum at very low q2. *Physics Letters B*, 825:136878, 2 2022.

[44] Michael Schmelling. Averaging correlated data. *Physica Scripta*, 51:676–679, 6 1995.

[45] Diogo Boito, Oscar Cata, Maarten Golterman, Matthias Jamin, Kim Maltman, James Osborne, and Santiago Peris. A new determination of α_s from hadronic τ decays. *Phys. Rev. D*, 84:113006, 2011.

[46] A.V. Nesterenko. On the low–energy behavior of the adler function. *Nuclear Physics B - Proceedings Supplements*, 186:207–210, 1 2009.

[47] G. Parisi. XI. The Borel transform and the renormalization group. *Physics Reports*, 49:215–219, 1 1979.

[48] David J. Griffiths. *Introduction to elementary particles*. Wiley-VCH, 2017.

[49] Bogoliubov N. N. and D. V. Shirkov. *Introduction to the theory of Quantized Fields*. John Wiley, 1980.

[50] Walter Greiner, Stefan Schramm, and Eckart Stein. *Quantum Chromodynamics*. Springer Berlin Heidelberg, 2007.

[51] Matthew D. Schwartz. *Quantum Field Theory and the Standard Model*. Cambridge University Press, 12 2013.